Large-deflection and post-buckling analyses of laminated composite beams by Carrera Unified Formulation

Large-deflection and post-buckling analyses of laminated composite beams by Carrera Unified Formulation

A. Pagani*, E. Carrera

Mul^2, Department of Mechanical and Aerospace Engineering
Politecnico di Torino
Corso Duca degli Abruzzi 24, 10129 Torino, Italy

Abstract: The Carrera Unified Formulation (CUF) was recently extended to deal with the geometric nonlinear analysis of solid cross-section and thin-walled metallic beams [1]. The promising results provided enough confidence for exploring the capabilities of that methodology when dealing with large displacements and post-buckling response of composite laminated beams, which is the subject of the present work. Accordingly, by employing CUF, governing nonlinear equations of low- to higher-order beam theories for laminated beams are expressed in this paper as degenerated cases of the three-dimensional elasticity equilibrium via an appropriate index notation. In detail, although the provided equations are valid for any one-dimensional structural theory in a unified sense, layer-wise kinematics are employed in this paper through the use of Lagrange polynomial expansions of the primary mechanical variables. The principle of virtual work and a finite element approximation are used to formulate the governing equations in a *total Lagrangian* manner, whereas a Newton-Raphson linearization scheme along with a path-following method based on the arc-length constraint is employed to solve the geometrically nonlinear problem. Several numerical assessments are proposed, including post-buckling of symmetric cross-ply beams and large displacement analysis of asymmetric laminates under flexural and compression loadings.

Keywords: Carrera unified formulation; Composite beams; Higher-order theories; Geometrical nonlinearities; Post-buckling; Path-following methods.

---

1 Introduction

During the last decades, composite laminates have been widely used for the design of advanced structural components. Even today, thanks to the new aircraft programs such as the Airbus A350XWB, aerospace industry continues to belong to the forerunners of composites application, manufacturing, and verification. As a natural consequence, contextually, research engineers and scientists have developed a large number of theories for describing the *rheological* behavior of composite structures and for substituting those obsolete models that were originally devised for metallic components. Interested readers can find more details about the modeling and linear mechanics of composite laminates for plate/shell and beam structures in

*Corresponding author. E-mail: alfonso.pagani@polito.it

the comprehensive review works by Carrera [2] and Kapania and Raciti [3, 4], respectively. Nevertheless, among the fundamental topics in structural mechanics, the *geometrical nonlinear analysis* of elastic structures holds a relevant importance. It is a matter of fact that the effects of large displacements and rotations may play a primary role in the correct prediction, for example, of flexible beams, which continue to be employed for wing structures, space antennas, rotor blades, and robotic arms. The literature about this argument is large, and a detailed discussion on nonlinear formulations of composite structures falls outside the scope of this work. However, some relevant papers on nonlinear beam models are briefly outlined hereinafter for the sake of completeness.

It is well known that for thin and solid cross-section beam structures, a good model for geometrically nonlinear analysis is represented by the so-called *elastica* [5, 6, 7]. The elastica beam addresses flexural problems by assuming the local curvature as proportional to the bending moment, according to the classical Euler-Bernoulli beam theory [8]. This assumption, of course, is too limiting for the analysis of composite structures, for which the shear effects may considerably alter the solution accuracy. For this reason, many works in the literature are based on the Timoshenko beam theory [9], which assumes a uniform shear distribution along the cross-section of the beam. In the domain of nonlinear analysis of metallic beams, this theory was extensively exploited; see for example the pioneering work of Reissner [10], who considered the effect of transverse force strains along with the principle of virtual work for the analysis of thin curved beams. The same author discussed the problem of coupled bending torsion deformation of beams in [11, 12].

The extension of the Timoshenko beam theory to the analysis of laminates is known to as First-order Shear Deformation Theory (FSDT). This model has been widely adopted for the finite displacements/rotations analysis of composite beams. For example, Kapania and Raciti [13] developed a simple one-dimensional finite element for the nonlinear analysis of symmetrically and asymmetrically laminated composite beams including shear deformation, bending-stretching coupling, and twisting. In contrast, the existing statically exact beam finite element based on FSDT was recently used to study the geometric nonlinear effects on static and dynamic responses in isotropic, composite and functionally graded material beams by Agarwal *et al.* [14]. Gupta *et al.* [15] presented a formulation for the post-buckling behavior of composite beams with axially immovable ends using the Rayleigh-Ritz method. Furthermore, Lanc *et al.* [16] discussed a beam finite element model for post-buckling analysis of composite laminated structures in the framework of an *updated Lagrangian* incremental formulation. In this work, the cross-section mid-line contour was assumed to remain undeformed in its plane, and the shear strains of the middle surface were neglected, according to classical lamination theory. Based on the Timoshenko's assumptions, instead, Li *et al.* [17] addressed buckling and post-buckling behaviors of laminated composite slender beams; also, an exact closed-form solution of elliptical integral form was provided in the same work. Large static deflection, mechanical and thermal buckling, post-buckling and nonlinear free vibration of laminated composite beams with surface bonded piezoelectric fiber reinforced composite layers were studied by Mareishi *et al.* [18]. Here, the governing equations of the piezoelectric fibre-reinforced laminated composite beams were derived based on Euler-Bernoulli beam theory and geometric nonlinearity of von Kármán. Finally, Kurtaran [19] focussed on geometrically nonlinear transient analysis of thick deep laminated composite curved beams by generalized differential quadrature method. In this paper, the Green-Lagrange nonlinear strain-displacement relations were considered along with FSDT assumptions.

The adoption of refined kinematics for the formulation of nonlinear beam models of composite laminates may be necessary when higher-order phenomena play an important role,

such as in the case of bending-torsion and axial-bending couplings, or when accurate stress analysis in the range of large displacements is needed. Inherently, Obst and Kapania [20] implemented a geometrical nonlinear beam model accounting for parabolic shear strain distribution through the thickness and satisfying the shear stress-free boundary conditions at the upper and lower free surfaces. Moreover, Singh *et al.* [21] studied the nonlinear bending behavior of asymmetric laminated composite beams using von Kármán large deflection theory and higher-order one-dimensional finite element having twelve degrees of freedom per node. Chandrashekhara and Bangera [22] carried out flexural analyses of fibre-reinforced composite beams through a higher-order shear deformation formulation. On the other hand, a generalized Vlasov theory for composite beams with arbitrary geometric and material sectional properties was systematically developed based on the Variational Asymptotic Beam Sectional (VABS) analysis in many papers, such as in [23]. In this work, instead of invoking ad-hoc kinematic assumptions, the variational-asymptotic method was used to split the geometrically nonlinear, three-dimensional elasticity problem into a linear, two-dimensional, cross-sectional analysis and a nonlinear, one-dimensional, beam analysis. Krawczyk *et al.* [24] and Krawczyk and Rebora [25] proposed a Layer-Wise (LW) beam model for geometric nonlinear finite element analysis of laminated beams with partial layer interaction and by assuming first-order shear deformations at layer level. The nonlinear response of composite beams modeled according to higher-order shear deformation theories in post-buckling was also investigated recently by Emam [26], by using Hamilton's principle and accounting for the contribution of the mid-plane stretching. Another relevant contribution is the one of Vidal and Polit [27], who developed a three-noded beam finite element for the nonlinear analysis of laminated beams based on a sinus distribution with layer refinement. The transverse shear strain was here obtained by using a cosine function avoiding the use of shear correction factors and ensuring the interlaminar continuity conditions on the interfaces between layers. Furthermore, Li and Qiao [28] extended the Reddy's high-order shear deformation beam theory with a von Kármán-type of kinematic nonlinearity for thermal post-buckling analysis of anisotropic laminated beams with different boundary conditions resting on two-parameter elastic foundations. In a work of the same authors [29] and in [30], the same formulation was also utilized for the analysis of beams with initial imperfections and composite tubular structures. As a final example, moreover, Mororó *et al.* [31] recently proposed a total Lagrangian formulation for the large displacements/moderated rotations analysis of thin-walled laminated beams. The constitutive matrix of the laminated beams was evaluated through an *ad-hoc* thin-walled beam theory in this work.

Although not comprehensive, this introductory review reveals a vivid interest in the subject. In this context, the present research wants to introduce a unified beam formulation able to deal with large displacement/rotation analysis of composite laminated beams accounting for higher-order effects, which include (but are not limited to) complex shear deformations, bending-torsion coupling, accurate post-buckling, and nonlinear three-dimensional stress/strain state analysis. The proposed geometrical nonlinear formulation is based on the Carrera Unified Formulation (CUF) [32, 33], which was recently extended to the nonlinear analysis of metallic beams by the same authors [1]. According to CUF, which assumes that any theory of structures can degenerate into a generalized kinematics by using an appropriate arbitrary expansion of the generalized variables, the nonlinear governing equations and the related finite element arrays of the generic, and eventually hierarchical, geometrically-exact composite beam theory are written in terms of *fundamental nuclei*. These fundamental nuclei represent the basic building blocks that, when opportunely expanded, allow for the straightforward generation of low- and high-order finite beam elements.

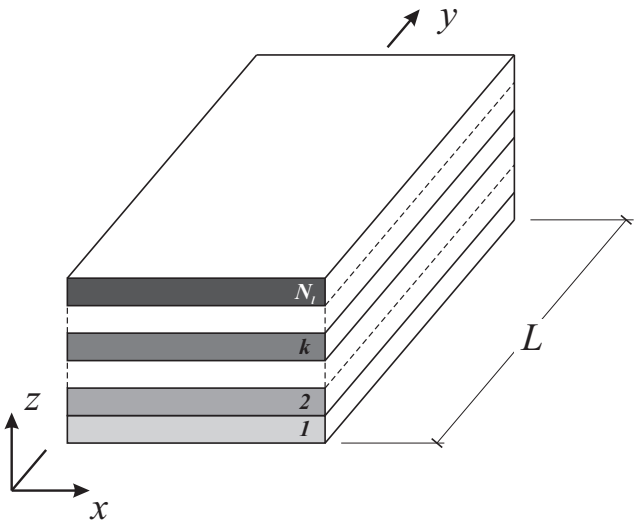

Figure 1: Laminated composite beam and related Cartesian coordinate frame.

In the present work, to ensure an appropriate description of the kinematics and to provide an enhanced accuracy at meso-scale, beam models with independent unknowns at the layer level are formulated by using Lagrange expansions of the primary variables, in a LW sense. Thus, after some preliminary and introductory considerations are made, the governing equations of the higher-order CUF finite element are obtained via the principle of virtual work. Subsequently, a linearized, incremental resolution technique with a path-following constraint is discussed. Also, this paper provides the explicit forms of the secant and tangent stiffness matrices of the unified element for laminated beams. Finally, several numerical results, including post-buckling of symmetric cross-ply beams and large displacement analysis of asymmetric laminates under flexural and compression loadings, are discussed to prove the efficacy of the present method.

2 Unified finite beam element

2.1 Preliminary considerations

Figure 1 shows a representative N_l-layered composite beam structure of length L and the related Cartesian coordinate system. The vector containing the three-dimensional displacement components of a given point in the structural domain is

$$\mathbf{u}(x,y,z) = \left\{ \begin{array}{ccc} u_x & u_y & u_z \end{array} \right\}^T \tag{1}$$

Accordingly, the stress ($\boldsymbol{\sigma}$) and strain ($\boldsymbol{\epsilon}$) states are expressed in the following vectorial form:

$$\begin{aligned} \boldsymbol{\sigma} &= \left\{ \begin{array}{cccccc} \sigma_{yy} & \sigma_{xx} & \sigma_{zz} & \sigma_{xz} & \sigma_{yz} & \sigma_{xy} \end{array} \right\}^T \\ \boldsymbol{\epsilon} &= \left\{ \begin{array}{cccccc} \epsilon_{yy} & \epsilon_{xx} & \epsilon_{zz} & \epsilon_{xz} & \epsilon_{yz} & \epsilon_{xy} \end{array} \right\}^T \end{aligned} \tag{2}$$

In this work, we consider each layer to be made of linear elastic monoclinic material in the plane xy (e.g., orthotropic fiber-matrix lamina with fiber orientation angle equal to θ with respect to the z-axis). In this case, the constitutive equations at layer level hold

$$\boldsymbol{\sigma} = \tilde{\mathbf{C}}\boldsymbol{\epsilon} \tag{3}$$

where the material matrix $\tilde{\mathbf{C}}$ is

$$\tilde{\mathbf{C}} = \begin{bmatrix} \tilde{C}_{11} & \tilde{C}_{12} & \tilde{C}_{13} & 0 & 0 & \tilde{C}_{16} \\ & \tilde{C}_{22} & \tilde{C}_{23} & 0 & 0 & \tilde{C}_{26} \\ & & \tilde{C}_{33} & 0 & 0 & \tilde{C}_{36} \\ & & & \tilde{C}_{44} & \tilde{C}_{45} & 0 \\ & & & & \tilde{C}_{55} & 0 \\ & \text{sym.} & & & & \tilde{C}_{66} \end{bmatrix} \tag{4}$$

The material coefficients $\tilde{C}_{ij}$ are functions of the elastic moduli along the longitudinal direction and the transverse directions of the fiber, the shear moduli, the Poisson ratios, and the fibre orientation angle. For the sake of brevity, their expressions are not given here but can be found in many reference texts, such as [34].

As far as the geometrical relations are concerned, the Green-Lagrange nonlinear strain components are considered. Therefore, the displacement-strain relations are expressed as

$$\boldsymbol{\epsilon} = \boldsymbol{\epsilon}_l + \boldsymbol{\epsilon}_{nl} = (\mathbf{b}_l + \mathbf{b}_{nl})\mathbf{u} \tag{5}$$

where $\mathbf{b}_l$ and $\mathbf{b}_{nl}$ are the linear and nonlinear differential operators, respectively. For the sake of completeness, these operators are given below.

$$\mathbf{b}_l = \begin{bmatrix} 0 & \partial_y & 0 \\ \partial_x & 0 & 0 \\ 0 & 0 & \partial_z \\ \partial_z & 0 & \partial_x \\ 0 & \partial_z & \partial_y \\ \partial_y & \partial_x & 0 \end{bmatrix}, \qquad \mathbf{b}_{nl} = \begin{bmatrix} \frac{1}{2}(\partial_y)^2 & \frac{1}{2}(\partial_y)^2 & \frac{1}{2}(\partial_y)^2 \\ \frac{1}{2}(\partial_x)^2 & \frac{1}{2}(\partial_x)^2 & \frac{1}{2}(\partial_x)^2 \\ \frac{1}{2}(\partial_z)^2 & \frac{1}{2}(\partial_z)^2 & \frac{1}{2}(\partial_z)^2 \\ \partial_x\,\partial_z & \partial_x\,\partial_z & \partial_x\,\partial_z \\ \partial_y\,\partial_z & \partial_y\,\partial_z & \partial_y\,\partial_z \\ \partial_x\,\partial_y & \partial_x\,\partial_y & \partial_x\,\partial_y \end{bmatrix} \tag{6}$$

where $\partial_x = \dfrac{\partial(\cdot)}{\partial x}$, $\partial_y = \dfrac{\partial(\cdot)}{\partial y}$, and $\partial_z = \dfrac{\partial(\cdot)}{\partial z}$.

2.2 Carrera Unified Formulation (CUF)

According to the Carrera Unified Formulation (CUF), the three-dimensional displacement field $\mathbf{u}(x, y, z)$ can be expressed as a general expansion of the primary unknowns. In the case of one-dimensional theories, one has:

$$\mathbf{u}(x, y, z) = F_\tau(x, z)\mathbf{u}_\tau(y), \qquad \tau = 1, 2, \cdots, M \tag{7}$$

where F_τ are the functions of the coordinates x and z on the cross-section, $\mathbf{u}_\tau$ is the vector of the *generalized* displacements which lay along the beam axis, M stands for the number of the terms used in the expansion, and the repeated subscript τ indicates summation. The choice of F_τ determines the class of the 1D CUF model that is required and subsequently to be adopted.

In this paper, Lagrange polynomials are used as F_τ cross-sectional functions. The resulting beam theories are known to as LE (Lagrange Expansion) CUF models in the literature [35]. In

detail, four-node bilinear (L4), nine-node quadratic (L9), and 16-node cubic (L16) expansions are used on each layer domain of the laminated beam in a layer-wise sense as outlined in [36]. In this manner, beam models with only pure displacements variables, layer-dependent unknowns, and piece-wise refined kinematics are formulated. Nevertheless, it is important to underline that, in the spirit of CUF, the governing equations discussed in this paper and the related methodology for solving the geometric nonlinear problem can be utilized with no loss of generality for the formulation of any other kind of higher-order beam model, including equivalent single-layer theories. The choice of adopting layer-wise formulation in the context of CUF in this work is driven by the enhanced accuracy these formulations provide at the *meso-scale*, especially in terms of stress distributions.

For the purpose of conciseness, LE F_τ expansions are not given in this paper. Interested readers can find more details on the use of LE in the context of CUF and for the formulation of layer-wise models in [35] and [36], respectively.

2.3 Finite element approximation

The Finite Element Method (FEM) is adopted to discretize the structure along the y-axis. Thus, the generalized displacement vector $\mathbf{u}_\tau(y)$ is approximated as follows:

$$\mathbf{u}_\tau(y) = N_i(y)\mathbf{q}_{\tau i} \qquad i = 1, 2, \ldots, p+1 \tag{8}$$

where N_i stands for the i-th shape function, p is the order of the shape functions and i indicates summation. $\mathbf{q}_{\tau i}$ is the following vector of the FE nodal parameters:

$$\mathbf{q}_{\tau i} = \left\{ \begin{array}{ccc} q_{x_{\tau i}} & q_{y_{\tau i}} & q_{z_{\tau i}} \end{array} \right\}^T \tag{9}$$

The shape functions N_i are not reported here. In this paper, we utilize classical four-node cubic finite elements. Their formal expressions can be found in fundamental book about finite elements, such as [37]. However, it should be underlined that the choice of the cross-section polynomials sets for the LE kinematics (i.e. the selection of the type, the number and the distribution of cross-sectional polynomials) is completely independent of the choice of the beam finite element to be used along the beam axis.

3 Nonlinear governing equations

3.1 Equilibrium

Equilibrium equations in the case of static analysis of layered beams are obtained here by using the principle of virtual work. It states that the sum of all the virtual work done by the internal and external forces existing in the system in any arbitrary infinitesimal virtual displacements satisfying the prescribed geometrical constraints is zero [38]. Namely,

$$\delta L_{\text{int}} - \delta L_{\text{ext}} = 0 \tag{10}$$

where L_{int} is the strain energy, L_{ext} is the work of the external loadings, and δ denotes the variation.

Large deflection analysis of elastic systems results in complex nonlinear differential problems, whose analytical solution is available rarely and limited to a narrow range of applications. The resolution of the geometrically nonlinear elasticity and related theories of structures can

be extended to a much wider class of problems if FEM is employed. In this case, in fact, the equilibrium condition of the structure can be expressed as a system of nonlinear algebraic equations. Moreover, if CUF (Eq. (7)) is utilized along with Eqs. (8) and (10), the equilibrium conditions and the related finite element arrays of the generic structural theory can be written in a simple and unified manner as follows:

$$\mathbf{K}_S^{ij\tau s}\,\mathbf{q}_{\tau i} - \mathbf{p}_{\tau i} = 0 \tag{11}$$

Equation (11) represents a set of three algebraic equations, where $\mathbf{p}_{\tau i}$ and $\mathbf{K}_S^{ij\tau s}$ are the Fundamental Nuclei (FNs) of the vector of the nodal loadings and the *secant* stiffness matrix, respectively. The derivation of the FN of the loading vector is not reported in this paper, but it can be found in [32]. On the other hand, the detailed formulation of the FN of the nonlinear secant stiffness matrix is discussed in Section 4.

Although the content of this section can be easily generalized to two-dimensional structural models (i.e., plates and shells) as well as three-dimensional elasticity, this paper primarily addresses beam theories based on CUF, according to which the finite element governing equations of the generic, arbitrary higher-order model can be automatically obtained by expanding Eq. (11) and the related FNs versus the indexes $\tau, s = 1, \cdots, M$ and $i, j = 1, \cdots, p+1$ to give

$$\mathbf{K}_S\,\mathbf{q} - \mathbf{p} = 0 \tag{12}$$

where $\mathbf{K}_S$, $\mathbf{q}$, and $\mathbf{p}$ are global, assembled finite element arrays of the final laminated beam structure. For more details about the expansion of the FNs and the finite element assembly procedure in the framework of CUF and in domain of linear mechanics, the readers are referred to the book by Carrera *et al.* [33].

3.2 Newton-Raphson method

Equation (12) constitutes the starting point for finite element calculation of geometrically nonlinear systems, and it is usually solved through an incremental linearized scheme, typically the Newton-Raphson method (or *tangent method*). According to the Newton-Raphson method, Eq. (12) is written as [39]:

$$\boldsymbol{\varphi}_{res} \equiv \mathbf{K}_S\,\mathbf{q} - \mathbf{p} = 0 \tag{13}$$

where $\boldsymbol{\varphi}_{res}$ is the vector of the *residual nodal forces* (unbalanced nodal force vector). Equation (13) can now be linearized by expanding $\boldsymbol{\varphi}_{res}$ in Taylor's series about a known solution $(\mathbf{q}, \mathbf{p})$. Omitting the second-order terms, one has

$$\boldsymbol{\varphi}_{res}(\mathbf{q}+\delta\mathbf{q}, \mathbf{p}+\delta\mathbf{p}) = \boldsymbol{\varphi}_{res}(\mathbf{q}, \mathbf{p}) + \frac{\partial \boldsymbol{\varphi}_{res}}{\partial \mathbf{q}}\,\delta\mathbf{q} + \frac{\partial \boldsymbol{\varphi}_{res}}{\partial \mathbf{p}}\,\delta\lambda\,\mathbf{p}_{ref} = 0 \tag{14}$$

where $\dfrac{\partial \boldsymbol{\varphi}_{res}}{\partial \mathbf{q}} = \mathbf{K}_T$ is the *tangent* stiffness matrix, and $-\dfrac{\partial \boldsymbol{\varphi}_{res}}{\partial \mathbf{p}}$ is equal to the unit matrix $\mathbf{I}$. In Eq. (14) it has been assumed that the load varies directly with the vector of the reference loadings $\mathbf{p}_{ref}$ and has a rate of change equal to the load parameter λ, i.e. $\mathbf{p} = \lambda\,\mathbf{p}_{ref}$. Equation (14) is written in a more compact form as follows:

$$\mathbf{K}_T\,\delta\mathbf{q} = \delta\lambda\,\mathbf{p}_{ref} - \boldsymbol{\varphi}_{res} \tag{15}$$

Since the load-scaling parameter λ is taken as a variable, an additional equation is required and this is given by a constraint relationship $c(\delta\mathbf{q}, \delta\lambda)$ to finally give

$$\begin{cases} \mathbf{K}_T\, \delta\mathbf{q} = \delta\lambda\, \mathbf{p}_{ref} - \boldsymbol{\varphi}_{res} \\ \\ c(\delta\mathbf{q}, \delta\lambda) = 0 \end{cases} \tag{16}$$

Depending on the constraint equation, different incremental schemes can be implemented. For example, if the constraint equation is $\delta\lambda = 0$, Eq. (16) corresponds to a *load-control method*. On the other hand, the condition $c(\delta\mathbf{q}, \delta\lambda) = \delta\mathbf{q} = 0$ represents a *displacement-control method*.

In this paper, a *path-following method* is employed in which the constraint equation is a function of both displacement and load parameter variations. More details about the differences between load- and displacement-control methods as well as path-following methods can be found in [39, 40, 41]. Essentially, we utilize the arc-length method as proposed by Criefield [42, 43] and then refined by Carrera [40], who devised a systematic solution based on the *consistent linearization* of the constraint equation for avoiding "doubling back" on the original load-deflection path. According to those fundamental works, the constraint relationship corresponds to a multi-dimensional sphere with radius equal to the given arch-length value Δl^0, which varies at each load step depending on the ratio of convergence at the previous iteration. A detailed discussion about the numerical iterative scheme employed for solving the gemetric nonlinear problem is not given in this paper, but it can be found in [1]. Nevertheless, it is important to clarify that we employ a *full* Newton-Raphson method that, as opposed to a *modified* scheme, utilizes an updated tangent stiffness matrix at each iteration. In contrast, the secant stiffness matrix is utilized for evaluating the equilibrium defect and the residual at each iteration, i.e. $\boldsymbol{\varphi}_{res}$. Therefore, by referring to a *total Lagrangian* formulation, the expressions of both $\mathbf{K}_S$ and $\mathbf{K}_T$ are provided in the following sections. These matrices are given in terms of FNs which, according to CUF, allow to engender the element matrices of any arbitrary refined and classical beam theories.

4 Derivation of the stiffness matrices

4.1 Fundamental nucleus of the secant stiffness matrix

The secant stiffness matrix $\mathbf{K}_S$ can be calculated from the virtual variation of the strain energy δL_{int}, which reads:

$$\delta L_{\text{int}} = < \delta\boldsymbol{\epsilon}^T \boldsymbol{\sigma} > \tag{17}$$

where $< (\cdot) >= \int_V (\cdot)\, dV$. Under the hypothesis of small deformations, V is the initial volume of the computational domain.

The strain vector $\boldsymbol{\epsilon}$ in Eq. (5) can be written in terms of the generalized nodal unknowns $\mathbf{u}_{\tau i}$ by employing Eqs. (7) and (8).

$$\boldsymbol{\epsilon} = (\mathbf{B}_l^{sj} + \mathbf{B}_{nl}^{sj})\mathbf{q}_{\tau i} \tag{18}$$

where $\mathbf{B}_l^{sj}$ and $\mathbf{B}_{nl}^{sj}$ are the two following matrices:

$$\mathbf{B}_l^{\tau i} = \mathbf{b}_l(F_\tau\, N_i) = \begin{bmatrix} 0 & F_\tau N_{i,y} & 0 \\ F_{\tau,x} N_i & 0 & 0 \\ 0 & 0 & F_{\tau,z} N_i \\ F_{\tau,z} N_i & 0 & F_{\tau,x} N_i \\ 0 & F_{\tau,z} N_i & F_\tau N_{i,y} \\ F_\tau N_{i,y} & F_{\tau,x} N_i & 0 \end{bmatrix} \tag{19}$$

and

$$\mathbf{B}_{nl}^{\tau i} = \frac{1}{2} \begin{bmatrix} u_{x,y} F_\tau N_{i,y} & u_{y,y} F_\tau N_{i,y} & u_{z,y} F_\tau N_{i,y} \\ u_{x,x} F_{\tau,x} N_i & u_{y,x} F_{\tau,x} N_i & u_{z,x} F_{\tau,x} N_i \\ u_{x,z} F_{\tau,z} N_i & u_{y,z} F_{\tau,z} N_i & u_{z,z} F_{\tau,z} N_i \\ u_{x,x} F_{\tau,z} N_i + u_{x,z} F_{\tau,x} N_i & u_{y,x} F_{\tau,z} N_i + u_{y,z} F_{\tau,x} N_i & u_{z,x} F_{\tau,z} N_i + u_{z,z} F_{\tau,x} N_i \\ u_{x,y} F_{\tau,z} N_i + u_{x,z} F_\tau N_{i,y} & u_{y,y} F_{\tau,z} N_i + u_{y,z} F_\tau N_{i,y} & u_{z,y} F_{\tau,z} N_i + u_{z,z} F_\tau N_{i,y} \\ u_{x,x} F_\tau N_{i,y} + u_{x,y} F_{\tau,x} N_i & u_{y,x} F_\tau N_{i,y} + u_{y,y} F_{\tau,x} N_i & u_{z,x} F_\tau N_{i,y} + u_{z,y} F_{\tau,x} N_i \end{bmatrix} \tag{20}$$

In Eqs. (19) and (20), commas denote partial derivatives. It is easy to verify that, analogously to Eq. (18), the virtual variation of the strain vector $\delta\boldsymbol{\epsilon}$ can be written in terms of nodal unknowns as follows:

$$\delta\boldsymbol{\epsilon} = \delta\big((\mathbf{B}_l^{sj} + \mathbf{B}_{nl}^{sj})\mathbf{q}_{sj}\big) = (\mathbf{B}_l^{sj} + 2\mathbf{B}_{nl}^{sj})\delta\mathbf{q}_{sj} \tag{21}$$

or, equivalently,

$$\delta\boldsymbol{\epsilon}^T = \delta\mathbf{q}_{sj}^T(\mathbf{B}_l^{sj} + 2\,\mathbf{B}_{nl}^{sj})^T \tag{22}$$

In writing Eqs. (21) and (22), the indexes s and j have been respectively used instead of τ and i for the sake of convenience.

Equations (3), (18) and (22) can now be substituted into Eq. (17) to have

$$\begin{aligned} \delta L_{\text{int}} &= \delta\mathbf{q}_{sj}^T < \left(\mathbf{B}_l^{sj} + 2\,\mathbf{B}_{nl}^{sj}\right)^T \mathbf{C}\left(\mathbf{B}_l^{\tau i} + \mathbf{B}_{nl}^{\tau i}\right) > \mathbf{q}_{\tau i} \\ &= \delta\mathbf{q}_{sj}^T\,\mathbf{K}_0^{ij\tau s}\,\mathbf{q}_{\tau i} + \delta\mathbf{q}_{sj}^T\,\mathbf{K}_{lnl}^{ij\tau s}\,\mathbf{q}_{\tau i} + \delta\mathbf{q}_{sj}^T\,\mathbf{K}_{nll}^{ij\tau s}\,\mathbf{q}_{\tau i} + \delta\mathbf{q}_{sj}^T\,\mathbf{K}_{nlnl}^{ij\tau s}\,\mathbf{q}_{\tau i} \\ &= \delta\mathbf{q}_{sj}^T\,\mathbf{K}_S^{ij\tau s}\,\mathbf{q}_{\tau i} \end{aligned} \tag{23}$$

where the secant stiffness matrix is $\mathbf{K}_S^{ij\tau s} = \mathbf{K}_0^{ij\tau s} + \mathbf{K}_{lnl}^{ij\tau s} + \mathbf{K}_{nll}^{ij\tau s} + \mathbf{K}_{nlnl}^{ij\tau s}$. In Eq. (23), $\mathbf{K}_0^{ij\tau s}$ is the linear component of $\mathbf{K}_S$ (i.e., it is the linear stiffness matrix), $\mathbf{K}_{lnl}^{ij\tau s}$ and $\mathbf{K}_{nll}^{ij\tau s}$ represent the nonlinear contributions of order 1, and $\mathbf{K}_{nlnl}^{ij\tau s}$ contains the nonlinearities of order 2. They are clearly given by:

$$\begin{aligned} \mathbf{K}_0^{ij\tau s} &=< (\mathbf{B}_l^{sj})^T\mathbf{C}\,\mathbf{B}_l^{\tau i} >\,, \qquad \mathbf{K}_{lnl}^{ij\tau s} =< (\mathbf{B}_l^{sj})^T\mathbf{C}\,\mathbf{B}_{nl}^{\tau i} > \\ \mathbf{K}_{nll}^{ij\tau s} &= 2 < (\mathbf{B}_{nl}^{sj})^T\mathbf{C}\,\mathbf{B}_l^{\tau i} >\,, \quad \mathbf{K}_{nlnl}^{ij\tau s} = 2 < (\mathbf{B}_{nl}^{sj})^T\mathbf{C}\,\mathbf{B}_{nl}^{\tau i} > \end{aligned} \tag{24}$$

For the sake of completeness, the expressions of matrices in Eq. (24) are given in Appendix A in the case of laminated beams. Matrices $\mathbf{K}_0^{ij\tau s}$, $\mathbf{K}_{lnl}^{ij\tau s}$, $\mathbf{K}_{nll}^{ij\tau s}$, and $\mathbf{K}_{nlnl}^{ij\tau s}$ are expressed

in terms of *fundamental nuclei*. These are 3×3 matrices that, given the cross-sectional functions ($F_\tau = F_s$, for $\tau = s$) and the shape functions ($N_i = N_j$, for $i = j$), can be expanded by using the indexes $\tau, s = 1, \cdots, M$ and $i, j = 1, \cdots, p+1$ in order to obtain the elemental secant stiffness matrix of any arbitrarily refined beam model. In other words, by opportunely choosing the beam kinematics (i.e., by choosing F_τ as well as the number of expansion terms M) low- to higher-order beam theories and related secant stiffness arrays can be implemented in an automatic manner by exploiting the index notation of CUF. Once the elemental secant stiffness matrix is obtained, it can be assembled in the classical way of FEM, see [33].

4.2 Fundamental nucleus of the tangent stiffness matrix

The fundamental nucleus of the tangent stiffness matrix $\mathbf{K}_T^{ij\tau s}$ is derived from the linearization of the equilibrium equations [44], see Eq. (14). We assume that the loading is conservative so that the linearization of the virtual variation of the external loads is null, i.e. $\delta(\delta L_{\text{ext}}) = 0$. Thus, the only terms to be linearized are the strain-displacement operators and the stress-strain relations. In fact, the tangent matrix can be formally obtained from linearizing the virtual variation of the strain energy as follows:

$$\begin{aligned} \delta(\delta L_{\text{int}}) &= < \delta(\delta \boldsymbol{\epsilon}^T \boldsymbol{\sigma}) > \\ &= < \delta \boldsymbol{\epsilon}^T \delta \boldsymbol{\sigma} > + < \delta(\delta \boldsymbol{\epsilon}^T) \boldsymbol{\sigma} > \\ &= \delta \mathbf{q}_{sj}^T (\mathbf{K}_0^{ij\tau s} + \mathbf{K}_{T_1}^{ij\tau s} + \mathbf{K}_\sigma^{ij\tau s}) \delta \mathbf{q}_{\tau i} \\ &= \delta \mathbf{q}_{sj}^T \mathbf{K}_T^{ij\tau s} \delta \mathbf{q}_{\tau i} \end{aligned} \tag{25}$$

Each nonlinear contribution in the right-hand-side of Eq. (25), i.e. $\mathbf{K}_{T_1}^{ij\tau s}$ and $\mathbf{K}_\sigma^{ij\tau s}$, is now considered separately. The first term, $< \delta \boldsymbol{\epsilon}^T \delta \boldsymbol{\sigma} >$, demands for the linearization of the constitutive relations (Eq. (3)), which, under the hypothesis of constant material coefficients (i.e., $\delta \mathbf{C} = 0$) and according to Eq. (21), hold

$$\delta \boldsymbol{\sigma} = \delta(\mathbf{C}\boldsymbol{\epsilon}) = \mathbf{C} \delta \boldsymbol{\epsilon} = \mathbf{C}(\mathbf{B}_l^{\tau i} + 2\,\mathbf{B}_{nl}^{\tau i}) \delta \mathbf{q}_{\tau i} \tag{26}$$

Hence, considering Eqs. (22) and (26), one has:

$$\begin{aligned} < \delta \boldsymbol{\epsilon}^T \delta \boldsymbol{\sigma} > &= \delta \mathbf{q}_{sj}^T < (\mathbf{B}_l^{sj} + 2\,\mathbf{B}_{nl}^{sj})^T \mathbf{C}\, (\mathbf{B}_l^{\tau i} + 2\,\mathbf{B}_{nl}^{\tau i}) > \delta \mathbf{q}_{\tau i} \\ &= \delta \mathbf{q}_{sj}^T\, \mathbf{K}_0^{ij\tau s}\, \delta \mathbf{q}_{\tau i} + \delta \mathbf{q}_{sj}^T \left(2\,\mathbf{K}_{lnl}^{ij\tau s}\right) \delta \mathbf{q}_{\tau i} + \delta \mathbf{q}_{sj}^T\, \mathbf{K}_{nll}^{ij\tau s}\, \delta \mathbf{q}_{\tau i} + \delta \mathbf{q}_{sj}^T \left(2\,\mathbf{K}_{nlnl}^{ij\tau s}\right) \delta \mathbf{q}_{\tau i} \\ &= \delta \mathbf{q}_{sj}^T \left(\mathbf{K}_0^{ij\tau s} + \mathbf{K}_{T_1}^{ij\tau s}\right) \delta \mathbf{q}_{\tau i} \end{aligned} \tag{27}$$

where $\mathbf{K}_{T_1}^{ij\tau s} = 2\,\mathbf{K}_{lnl}^{ij\tau s} + \mathbf{K}_{nll}^{ij\tau s} + 2\,\mathbf{K}_{nlnl}^{ij\tau s}$ is the nonlinear contribution of the fundamental nucleus of the tangent stiffness matrix due to the linearization of the Hooke's law.

The evaluation of the second contribution in the right-hand-side of Eq. (25), i.e. $< \delta(\delta \boldsymbol{\epsilon}^T) \boldsymbol{\sigma} >$, requires the linearization of the nonlinear geometric relations. According to Crisfield [41] and from Eqs. (5) and (6), one can verify that the linearization of the virtual

variation of the strain vector holds

$$\delta(\delta\boldsymbol{\epsilon}) = \left\{ \begin{array}{c} \left(\delta u_{x_{,x}}\right)_{\mathrm{v}} \delta u_{x_{,x}} + \left(\delta u_{y_{,x}}\right)_{\mathrm{v}} \delta u_{y_{,x}} + \left(\delta u_{z_{,x}}\right)_{\mathrm{v}} \delta u_{z_{,x}} \\ \left(\delta u_{x_{,y}}\right)_{\mathrm{v}} \delta u_{x_{,y}} + \left(\delta u_{y_{,y}}\right)_{\mathrm{v}} \delta u_{y_{,y}} + \left(\delta u_{z_{,y}}\right)_{\mathrm{v}} \delta u_{z_{,y}} \\ \left(\delta u_{x_{,z}}\right)_{\mathrm{v}} \delta u_{x_{,z}} + \left(\delta u_{y_{,y}}\right)_{\mathrm{v}} \delta u_{y_{,z}} + \left(\delta u_{z_{,z}}\right)_{\mathrm{v}} \delta u_{z_{,z}} \\ \left[\left(\delta u_{x_{,x}}\right)_{\mathrm{v}} \delta u_{x_{,z}} + \delta u_{x_{,x}} \left(\delta u_{x_{,z}}\right)_{\mathrm{v}}\right] + \left[\left(\delta u_{y_{,x}}\right)_{\mathrm{v}} \delta u_{y_{,z}} + \delta u_{y_{,x}} \left(\delta u_{y_{,z}}\right)_{\mathrm{v}}\right] + \left[\left(\delta u_{z_{,x}}\right)_{\mathrm{v}} \delta u_{z_{,z}} + \delta u_{z_{,x}} \left(\delta u_{z_{,z}}\right)_{\mathrm{v}}\right] \\ \left[\left(\delta u_{x_{,y}}\right)_{\mathrm{v}} \delta u_{x_{,z}} + \delta u_{x_{,y}} \left(\delta u_{x_{,z}}\right)_{\mathrm{v}}\right] + \left[\left(\delta u_{y_{,y}}\right)_{\mathrm{v}} \delta u_{y_{,z}} + \delta u_{y_{,y}} \left(\delta u_{y_{,z}}\right)_{\mathrm{v}}\right] + \left[\left(\delta u_{z_{,y}}\right)_{\mathrm{v}} \delta u_{z_{,z}} + \delta u_{z_{,y}} \left(\delta u_{z_{,z}}\right)_{\mathrm{v}}\right] \\ \left[\left(\delta u_{x_{,x}}\right)_{\mathrm{v}} \delta u_{x_{,y}} + \delta u_{x_{,x}} \left(\delta u_{x_{,y}}\right)_{\mathrm{v}}\right] + \left[\left(\delta u_{y_{,x}}\right)_{\mathrm{v}} \delta u_{y_{,y}} + \delta u_{y_{,x}} \left(\delta u_{y_{,y}}\right)_{\mathrm{v}}\right] + \left[\left(\delta u_{z_{,x}}\right)_{\mathrm{v}} \delta u_{z_{,y}} + \delta u_{z_{,x}} \left(\delta u_{z_{,y}}\right)_{\mathrm{v}}\right] \end{array} \right\} \tag{28}$$

where the subscript "v" denotes the variations. It is easy to justify the following matricial form of Eq. (28) by employing CUF (7) and the finite element approximation (8) for both the linearized variables (i.e., $\delta\mathbf{u} = F_\tau N_i \delta\mathbf{q}_{\tau i}$) and the variations (i.e., $(\delta\mathbf{u})_{\mathrm{v}} = F_s N_j \delta\mathbf{q}_{sj}$):

$$\delta(\delta\boldsymbol{\epsilon}) = \mathbf{B}^*_{nl} \left\{ \begin{array}{c} \delta q_{x_{\tau i}} \delta q_{x_{sj}} \\ \delta q_{y_{\tau i}} \delta q_{y_{sj}} \\ \delta q_{z_{\tau i}} \delta q_{z_{sj}} \end{array} \right\} \tag{29}$$

or rather

$$\delta(\delta\boldsymbol{\epsilon}^T) = \left\{ \begin{array}{c} \delta q_{x_{\tau i}} \delta q_{x_{sj}} \\ \delta q_{y_{\tau i}} \delta q_{y_{sj}} \\ \delta q_{z_{\tau i}} \delta q_{z_{sj}} \end{array} \right\}^T (\mathbf{B}^*_{nl})^T \tag{30}$$

where

$$\mathbf{B}^*_{nl} = \left[\begin{array}{ccc} F_{\tau_{,x}} F_{s_{,x}} N_i N_j & F_{\tau_{,x}} F_{s_{,x}} N_i N_j & F_{\tau_{,x}} F_{s_{,x}} N_i N_j \\ F_\tau F_s N_{i_{,y}} N_{j_{,y}} & F_\tau F_s N_{i_{,y}} N_{j_{,y}} & F_\tau F_s N_{i_{,y}} N_{j_{,y}} \\ F_{\tau_{,z}} F_{s_{,z}} N_i N_j & F_{\tau_{,z}} F_{s_{,z}} N_i N_j & F_{\tau_{,z}} F_{s_{,z}} N_i N_j \\ F_{\tau_{,x}} F_{s_{,z}} N_i N_j + F_{\tau_{,z}} F_{s_{,x}} N_i N_j & F_{\tau_{,x}} F_{s_{,z}} N_i N_j + F_{\tau_{,z}} F_{s_{,x}} N_i N_j & F_{\tau_{,x}} F_{s_{,z}} N_i N_j + F_{\tau_{,z}} F_{s_{,x}} N_i N_j \\ F_{\tau_{,z}} F_s N_i N_{j_{,y}} + F_\tau F_{s_{,z}} N_{i_{,y}} N_j & F_{\tau_{,z}} F_s N_i N_{j_{,y}} + F_\tau F_{s_{,z}} N_{i_{,y}} N_j & F_{\tau_{,z}} F_s N_i N_{j_{,y}} + F_\tau F_{s_{,z}} N_{i_{,y}} N_j \\ F_{\tau_{,x}} F_s N_i N_{j_{,y}} + F_\tau F_{s_{,x}} N_{i_{,y}} N_j & F_{\tau_{,x}} F_s N_i N_{j_{,y}} + F_\tau F_{s_{,x}} N_{i_{,y}} N_j & F_{\tau_{,x}} F_s N_i N_{j_{,y}} + F_\tau F_{s_{,x}} N_{i_{,y}} N_j \end{array} \right] \tag{31}$$

Given Eq. (30) and after simple manipulations, the following passages are fairly clear:

$$\begin{aligned} < \delta(\delta\boldsymbol{\epsilon}^T)\boldsymbol{\sigma} > &= < \left\{ \begin{array}{c} \delta q_{x_{\tau i}} \delta q_{x_{sj}} \\ \delta q_{y_{\tau i}} \delta q_{y_{sj}} \\ \delta q_{z_{\tau i}} \delta q_{z_{sj}} \end{array} \right\}^T (\mathbf{B}^*_{nl})^T \boldsymbol{\sigma} > \\ &= \delta\mathbf{q}^T_{sj} < \mathrm{diag}\left((\mathbf{B}^*_{nl})^T \boldsymbol{\sigma}\right) > \delta\mathbf{q}_{\tau i} \\ &= \delta\mathbf{q}^T_{sj} < \mathrm{diag}\left((\mathbf{B}^*_{nl})^T (\boldsymbol{\sigma}_l + \boldsymbol{\sigma}_{nl})\right) > \delta\mathbf{q}_{\tau i} \\ &= \delta\mathbf{q}^T_{sj} (\mathbf{K}^{ij\tau s}_{\sigma_l} + \mathbf{K}^{ij\tau s}_{\sigma_{nl}}) \delta\mathbf{q}_{\tau i} = \delta\mathbf{q}^T_{sj} \mathbf{K}^{ij\tau s}_{\sigma} \delta\mathbf{q}_{\tau i} \end{aligned} \tag{32}$$

where $\mathrm{diag}\left((\mathbf{B}^*_{nl})^T \boldsymbol{\sigma}\right)$ is the 3×3 diagonal matrix, whose diagonal terms are the components of the vector $(\mathbf{B}^*_{nl})^T \boldsymbol{\sigma}$. According to Eqs. (3) and (5), $\boldsymbol{\sigma}_l = \mathbf{C}\boldsymbol{\epsilon}_l$ and $\boldsymbol{\sigma}_{nl} = \mathbf{C}\boldsymbol{\epsilon}_{nl}$. The term elaborated in Eq. (32) defines a contribution of the tangent stiffness arising from the nonlinear

form of the strain-displacement equations and is often called the geometric stiffness [44], of which $\mathbf{K}_{\sigma}^{ij\tau s} = \mathbf{K}_{\sigma_l}^{ij\tau s} + \mathbf{K}_{\sigma_{nl}}^{ij\tau s}$ is the fundamental nucleus. The explicit form of $\mathbf{K}_{\sigma}^{ij\tau s}$ is given in the following for the sake of completeness:

$$\begin{aligned}
\mathbf{K}_{\sigma}^{ij\tau s} &= \big(< \sigma_{xx} F_{\tau,x} F_{s,x} N_i N_j > + < \sigma_{yy} F_{\tau} F_{s} N_{i,y} N_{j,x} > \\
&+ < \sigma_{zz} F_{\tau,z} F_{s,z} N_i N_j > + < \sigma_{xy} F_{\tau,x} F_{s} N_i N_{j,y} > \\
&+ < \sigma_{xy} F_{\tau} F_{s,x} N_{i,y} N_j > + < \sigma_{xz} F_{\tau,x} F_{s,z} N_i N_j > \\
&+ < \sigma_{xz} F_{\tau,z} F_{s,x} N_i N_j > + < \sigma_{yz} F_{\tau,z} F_{s} N_i N_{j,y} > \\
&+ < \sigma_{yz} F_{\tau} F_{s,z} N_{i,y} N_j > \big) \, \mathbf{I}
\end{aligned} \tag{33}$$

where $\mathbf{I}$ is the 3×3 identity matrix. Given $\mathbf{K}_{T_1}^{ij\tau s}$ and $\mathbf{K}_{\sigma}^{ij\tau s}$, the fundamental nucleus of the tangent stiffness matrix $\mathbf{K}_{T}^{ij\tau s}$ can be calculated straightforwardly (see Eq. (25)). It is now clear that this 3×3 matrix is the basic building block to be used for the formulation of the tangent stiffness matrix for any higher-order refined beam elements accounting for Green-Lagrange nonlinear strains. Readers can easily verify that the expansion of the FN of the tangent stiffness results into a symmetric element matrix. It is intended that, depending on the problem, the formulation of the fundamental nuclei of the secant and tangent stiffness matrices is much simplified if only some geometrical nonlinearities are retained, such as in the case of von Kármán nonlinearities.

4.3 Symmetric form of the secant stiffness matrix

It is of relevant importance to note that $\mathbf{K}_S$ as given in Section 4.1 is not symmetric. The non-symmetry of the secant stiffness matrix may result in mathematical and practical drawbacks. In essence, this would seriously affect in a negative manner both the calculation times and the memory usage in the domain of FE methods. For this reason, in the past and recent literature, some authors have explored new possibilities of formulating symmetric forms of the secant stiffness matrix, see for example [45, 46, 47, 48, 49]. In the present work, and according to Carrera [50, 51], a symmetric form of the secant stiffness matrix is devised by expressing the virtual variation of the internal strain energy due by the contribution $\mathbf{K}_{nll}^{ij\tau s}$ as follows (see [1]):

$$\begin{aligned}
(\delta L_{\text{int}})_{nll} &= < \delta \, \boldsymbol{\epsilon}_{nl}^{T} \, \boldsymbol{\sigma}_{l} > \\
&= \frac{1}{2} < \delta \boldsymbol{\epsilon}_{nl}^{T} \, \mathbf{C} \, \boldsymbol{\epsilon}_{l} + \delta \boldsymbol{\epsilon}_{nl}^{T} \, \boldsymbol{\sigma}_{l} > \\
&= \frac{1}{2} \delta \mathbf{q}_{sj}^{T} (\mathbf{K}_{nll}^{ij\tau s} + \mathbf{K}_{\sigma_l}^{ij\tau s}) \mathbf{q}_{\tau i}
\end{aligned} \tag{34}$$

Thus, following Eq. (23), the total virtual variation of the strain energy is

$$\delta L_{\text{int}} = \delta \mathbf{q}_{sj}^{T} (\mathbf{K}_{0}^{ij\tau s} + \mathbf{K}_{lnl}^{ij\tau s} + \frac{1}{2} \mathbf{K}_{nll}^{ij\tau s} + \frac{1}{2} \mathbf{K}_{\sigma_l}^{ij\tau s} + \mathbf{K}_{nlnl}^{ij\tau s}) \mathbf{q}_{\tau i} \tag{35}$$

or, in other words,

$$\mathbf{K}_{S}^{ij\tau s} = \mathbf{K}_{0}^{ij\tau s} + \mathbf{K}_{lnl}^{ij\tau s} + \frac{1}{2} \mathbf{K}_{nll}^{ij\tau s} + \frac{1}{2} \mathbf{K}_{\sigma_l}^{ij\tau s} + \mathbf{K}_{nlnl}^{ij\tau s} = \mathbf{K}_{0}^{ij\tau s} + \frac{1}{2} (\mathbf{K}_{T1}^{ij\tau s} + \mathbf{K}_{\sigma_l}^{ij\tau s}) \tag{36}$$

The expansion of the fundamental nucleus of the secant stiffness matrix as given above results now into a symmetric matrix.

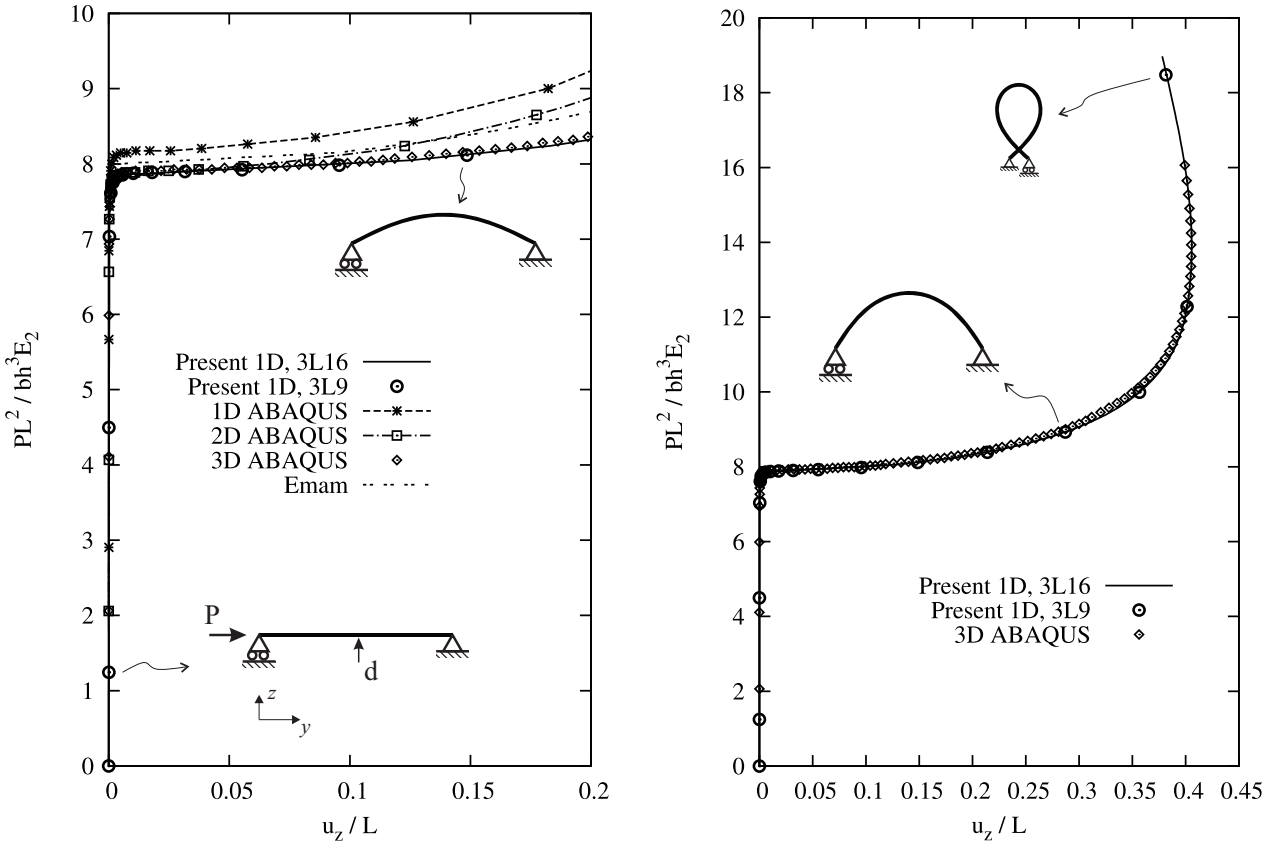

(a) Moderate displacements/rotations

(b) Large displacements/rotations

Figure 2: Post-buckling equilibrium curves and representative deformed states of the three-layer cross-ply beam in the range of moderate and large displacements/rotations.

5 Numerical results

In order to assess the enhanced capabilities of the present unified beam theory, post-buckling of symmetric cross-ply beams and large displacement analysis of asymmetric laminates under flexural and compression loadings are addressed. If not otherwise stated, all the CUF models employed make use of 20 cubic finite elements to approximate the solution field along the beam axis. Furthermore, all the reference FE solutions provided come from convergence analysis for ensuring a fair comparison in terms of both accuracy and computational costs.

5.1 Post-buckling of symmetric cross-ply beam

The first assessment deals with the post-buckling analysis of a symmetric cross-ply $[0°/90°/0°]$ beam structure. For representative purposes, the beam is long $L = 250$ mm. The beam cross-section is square with width $b = 5$ mm and total heigh $h = b$. Also, each of the three layers of the laminate has the same thickness and measures $t = h/3$. The laminae are made of an orthotropic material with the following characteristics: $E_1 = 155$ GPa, $E_2 = 15.5$ GPa, $G_{12} = G_{13} = 0.6\,E_2$, $G_{23} = 0.5\,E_2$, $\nu_{12} = 0.25$.

Post-buckling equilibrium curves are shown, in the case of simply-supported boundary conditions, in Fig. 2, where the vertical displacement component u_z at the midspan section is given as function of the applied compression load P in both moderate and large displacements/rotations ranges. In the same graphs, deformed configurations by the present 3L16

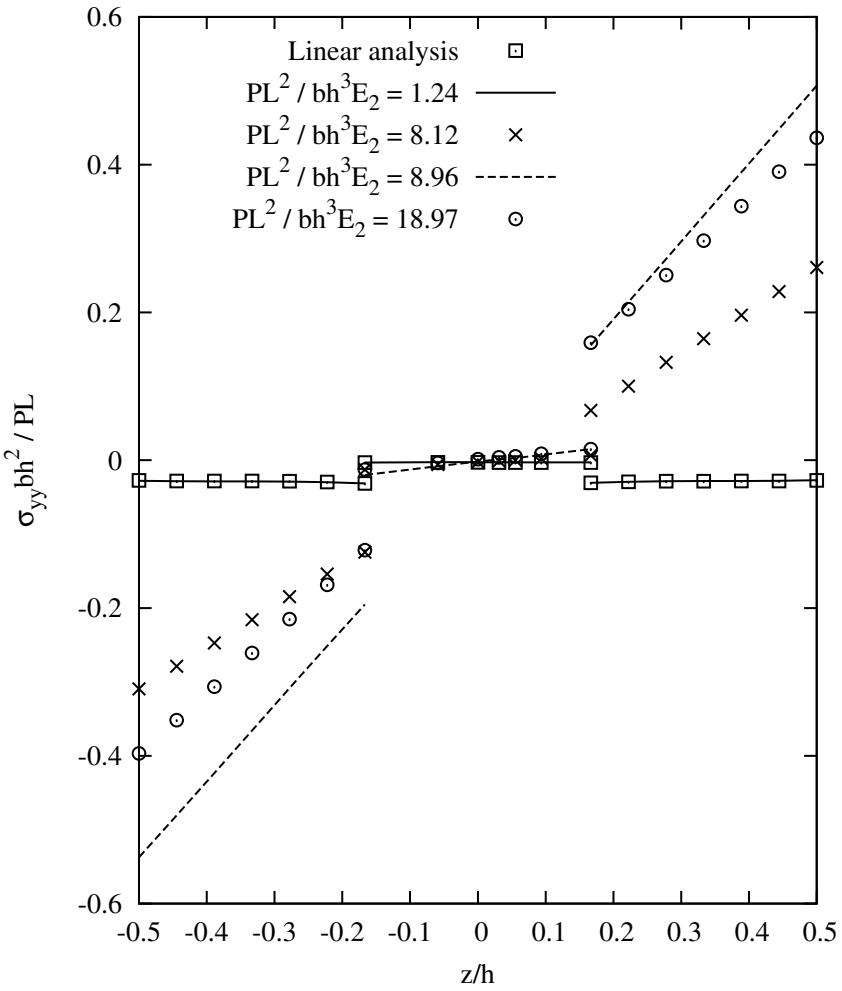

Figure 3: Through-the-thickness distribution of axial, σ_{yy}, stress component at $y = 0.1\,L$. 3L16 beam model.

CUF beam model at representative equilibrium states are depicted for the sake of completeness. In conducting this first analysis, a defect load $d = 0.2$ N is applied as in Fig. 2(a) to enforce the stable branch after the buckling load is reached. The figures compares the results from the present refined beam model with those from ABAQUS and from Emam [26], who utilized a higher-order shear deformation theory along with von Kármán nonlinearities for the post-buckling analysis of composite beams within the range of moderate displacements. It should be underlined that the proposed 3L9 and 3L16 beam models make use of piece-wise quadratic and cubic approximation of the displacement field, respectively. In other words, as an example, each layer of the composite laminate is modelled with a quadratic L9 Lagrange polynomial in the case of 3L9 beam model, in a layer-wise sense. On the contrary, 1D ABAQUS model is made of 50 B22 elements (606 Degrees of Freedom, DOFs); 2D ABAQUS utilizes 625 S8R plate elements ($\approx$ 13000 DOFs); and, finally, 3D ABAQUS model is built with 39600 C3D20 brick elements ($\approx$ 500000 DOFs). It is intended that the present 3L9 model has 3843 DOFs, whereas the 3L16 beam has 7320 DOFs.

Figure 3 shows the axial stress distribution along the thickness of the laminated beam close to the loaded end, at $y = 0.1\,L$. The results in this figure come from the present 3L16 beam model, whose accuracy in predicting accurate stress distributions is demonstrated in the next section. It is interesting to note that Fig. 3 reveals the compression nature of the

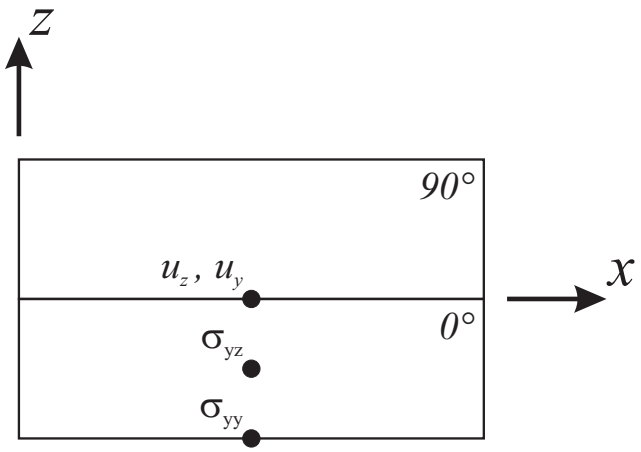

Figure 4: Cross-section and verification points of the two-layer asymmetric cross-ply beam.

problem under consideration in the linear range and for $\frac{PL^2}{bh^3E_2} < 7.88$, which is the value of the critical load according to the beam model of interest. On the other hand, the system clearly becomes dominated by flexure after the buckling load is attained.

This preliminary analysis shows the interesting capabilities of the proposed beam theories to deal with large displacement analysis and post-buckling of symmetric laminated structure. These CUF-based refined beam models, which employ three-dimensional Green-Lagrange strain/displacement relations within a total Lagrangian approach framework, are able to replicate 3D FEM models by ABAQUS with a very low number of DOFs. Also, the layer-wise behaviour of the in-plane axial stress components provides confidence for the effectiveness of the LE models in dealing with accurate stress/strain field description in linear and geometrical nonlinear ranges.

5.2 Large deflection of asymmetric beams subjected to bending and compression

The following analyses deal with the geometric nonlinear response of asymmetric laminated beams. The cross-ply two-layer [0°/90°] structure, whose cross-section is shown in Fig. 4, is considered in this example. Without affecting the generality of the analysis, each layer is $t = h/2 = 0.3$ m thick and is made of an orthotropic AS4/3501-6 graphite/epoxy material with the following properties: $E_1 = 144.8$ GPa, $E_2 = 9.65$ GPa, $G_{12} = G_{13} = 4.14$ GPa, $G_{23} = 3.45$ GPa, $\nu_{12} = 0.3$. The total length of the beam is $L = 9$ m and the section width is $b = 1$ m.

In the first loading case, the beam is subjected to clamped-free boundary conditions and undergoes a constant transverse load per unit of area equal to p_0. For clarity reasons, these boundary conditions are represented in Fig. 9, which also shows the linear and nonlinear equilibrium curves along with some representative deformed configurations of the structure by the present higher-order beam model. In the figure, the solutions by the bi-linear (2L4), quadratic (2L9), and cubic (2L16) layer-wise CUF models are compared with the one from an ABAQUS three-dimensional FEM model. Displacement and stress components for two illustrative loading values are also given in Table 1, for the sake of completeness. This table compares the vertical (u_z) and out-of-plane axial (u_y) displacements as well as axial normal (σ_{yy}) and transverse shear (σ_{yz}) stress components at some verification points of the structure domain (see Fig. 4) and between the present beam models and the 3D ABAQUS results. Also,

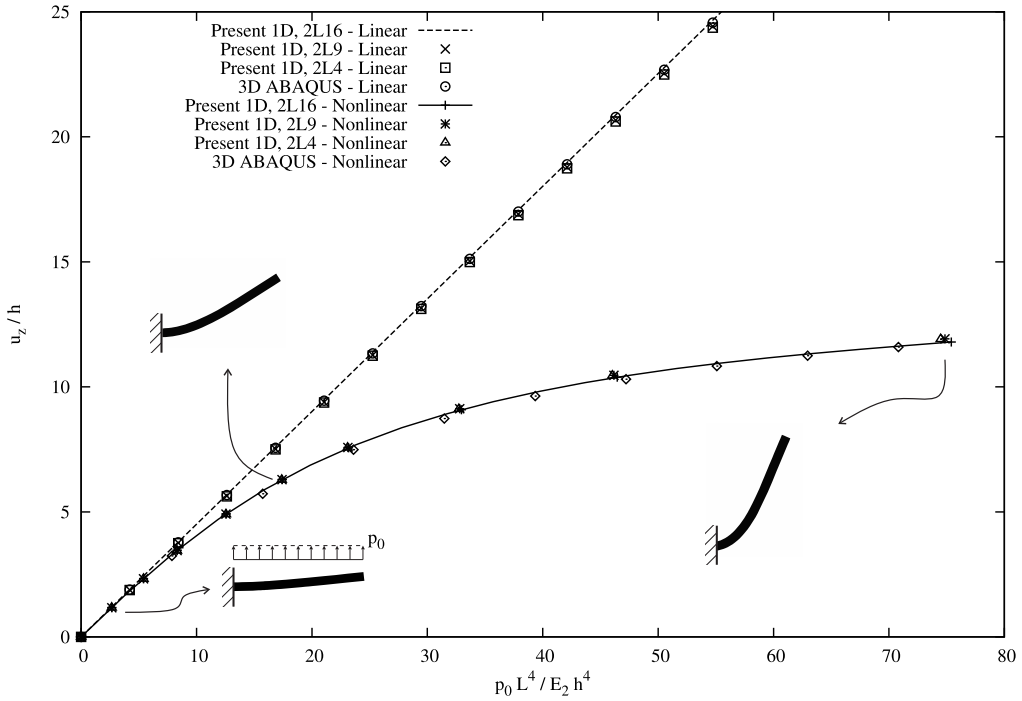

Figure 5: Equilibrium curves and representative deformed states of the two-layer cross-ply beam subjected to bending.

	$p_0 = 3 \times 10^6$ Pa				$p_0 = 9 \times 10^6$ Pa				
	u_z [m]	u_y [m]	σ_{yy} [MPa]	σ_{yz} [MPa]	u_z [m]	u_y [m]	σ_{yy} [MPa]	σ_{yz} [MPa]	DOFs
2L4	3.50	−0.88	1019.29	29.79	6.32	−3.17	1602.84	55.92	1098
2L9	3.51	−0.88	1003.84	29.44	6.32	−3.18	1573.42	55.22	2745
2L16	3.51	−0.99	1007.74	40.25	6.26	−3.37	1565.90	74.55	5124
ABAQUS 3D	3.43	−0.85	959.42	40.99	6.18	−3.02	1580.03	80.02	573675

Table 1: Displacement and stress components of the cantilever asymmetric cross-ply beam subjected to bending. Displacements and stresses are evaluated at $y = L$ and $y = L/2$, respectively, and in correspondence of the evaluation points, see Fig. 4.

the number of DOFs involved in the analysis are also highlighted per each model. Axial and shear stress components distributions along the beam thickness at the mid-span beam cross-section, $y = L/2$, are depicted in Figs. 6, 7, and 8 for both linear and nonlinear analyses. This analysis suggests the following comments:

- Both lower- and higher-order layer-wise CUF models are able to represent correctly – and in accordance with the 3D finite elements solution – the equilibrium path of asymmetric cross-ply beams subjected to large displacements.
- L4, L9 and L16 layer-wise kinematics are all adequate for capturing reliable solutions in terms of distribution of axial stress components.
- In order to describe correctly the quadratic piece-wise distribution of the transverse shear stresses, at least a cubic model (L16) is needed. This beam theory satisfy the continuity of the shear stresses through the thickness for both moderate and large loadings and is in good agreement with the 3D ABAQUS solution. On the contrary, the L4 and

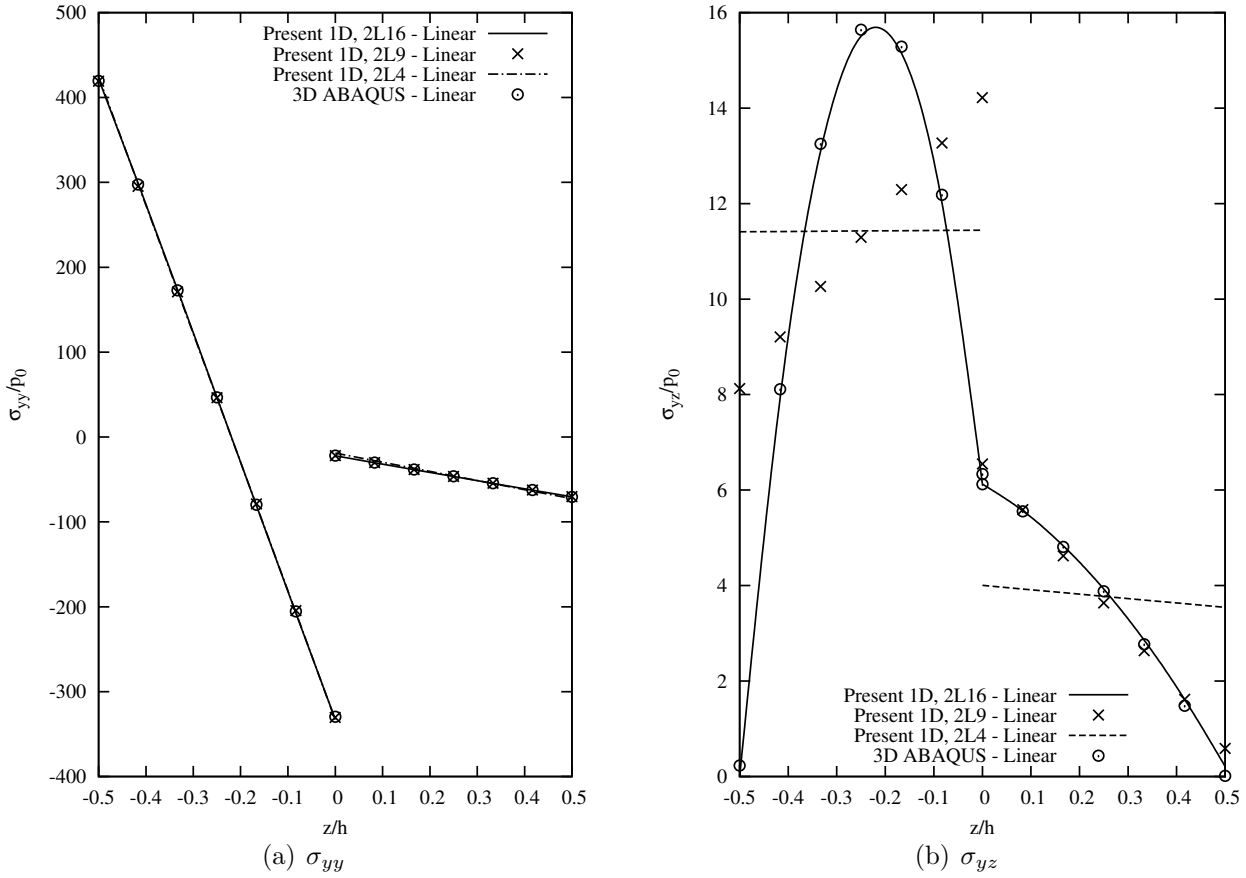

(a) σ_{yy} (b) σ_{yz}

Figure 6: Through-the-thickness distribution of axial, σ_{yy}, and transverse, σ_{yz}, stress components at the mid-span of the cantilever asymmetric cross-ply beam subjected to bending. Linear analysis.

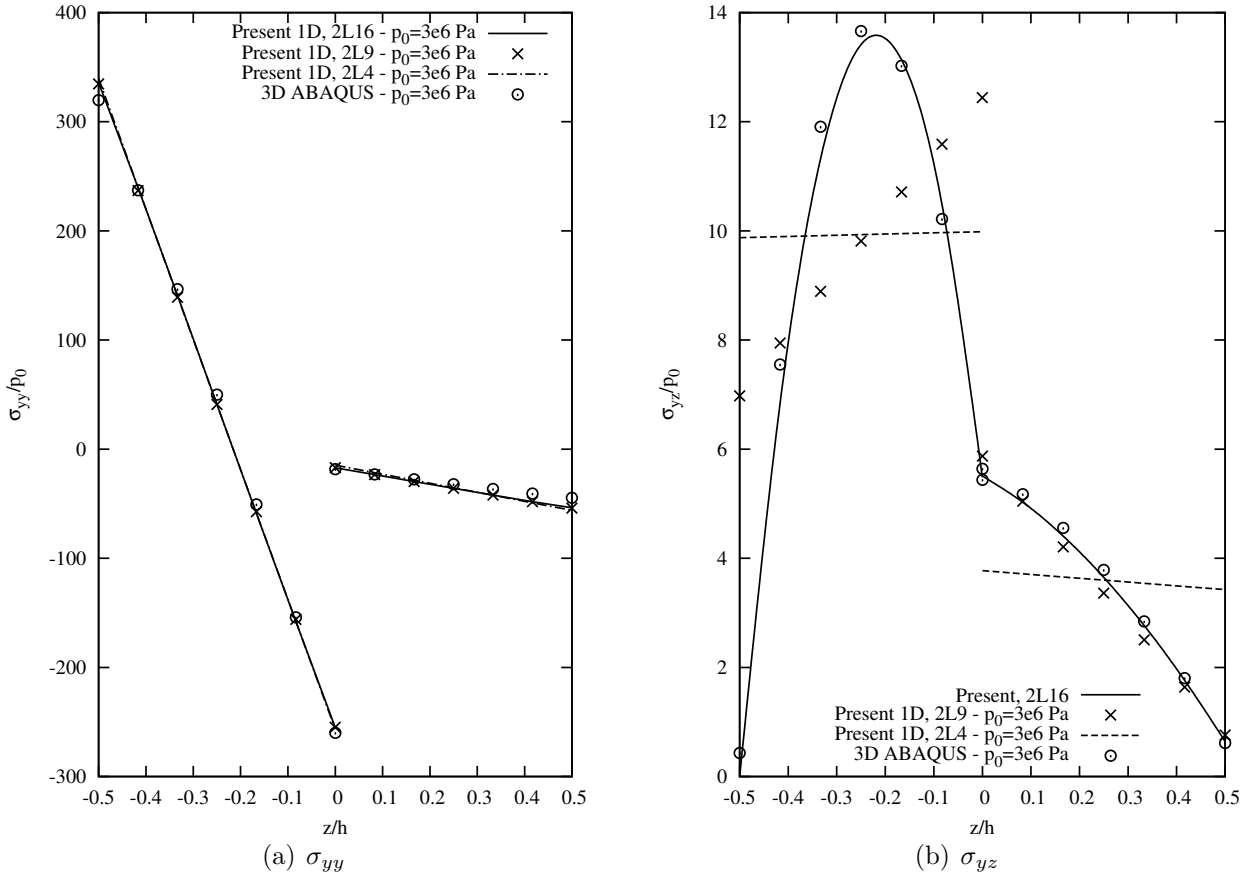

(a) σ_{yy} (b) σ_{yz}

Figure 7: Through-the-thickness distribution of axial, σ_{yy}, and transverse, σ_{yz}, stress components at the mid-span of the cantilever asymmetric cross-ply beam subjected to bending. Nonlinear analysis, $p_0 = 3 \times 10^6$ Pa.

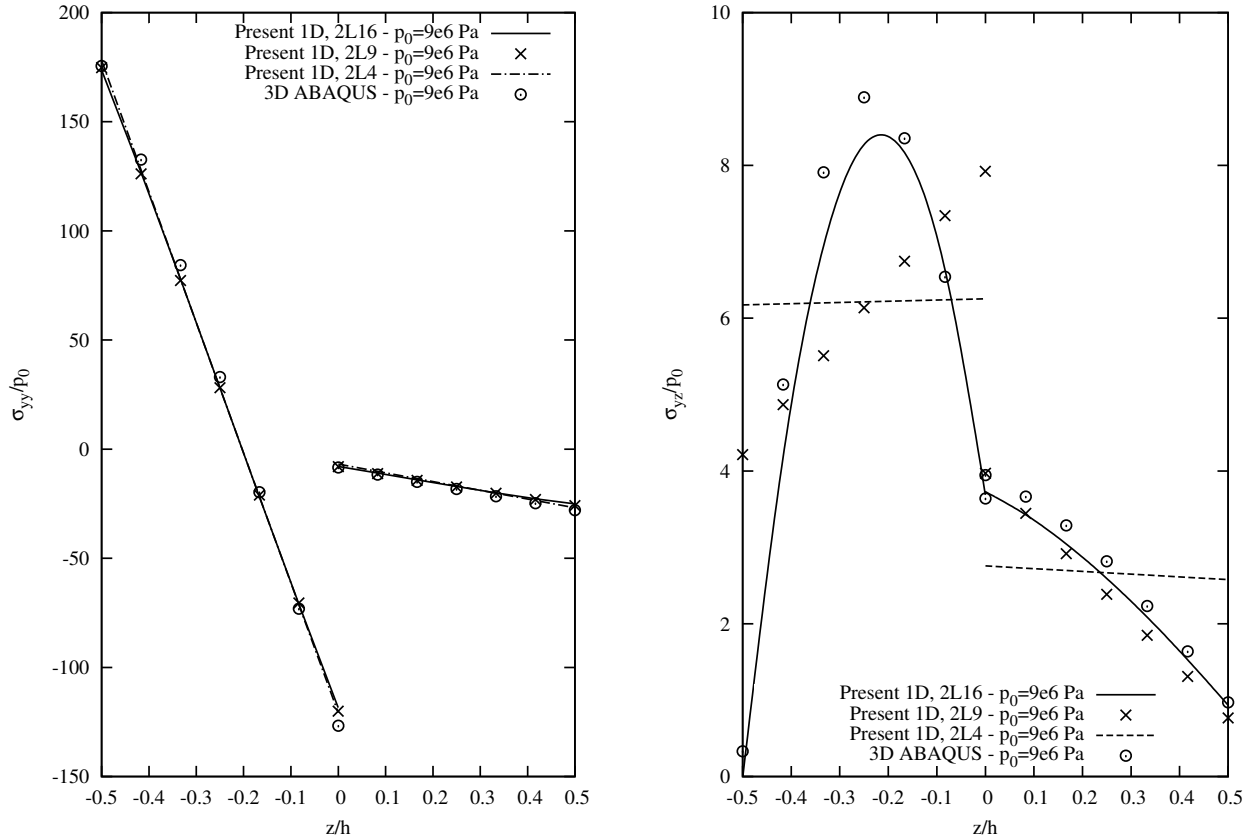

(a) σ_{yy} (b) σ_{yz}

Figure 8: Through-the-thickness distribution of axial, σ_{yy}, and transverse, σ_{yz}, stress components at the mid-span of the cantilever asymmetric cross-ply beam subjected to bending. Nonlinear analysis, $p_0 = 9 \times 10^6$ Pa.

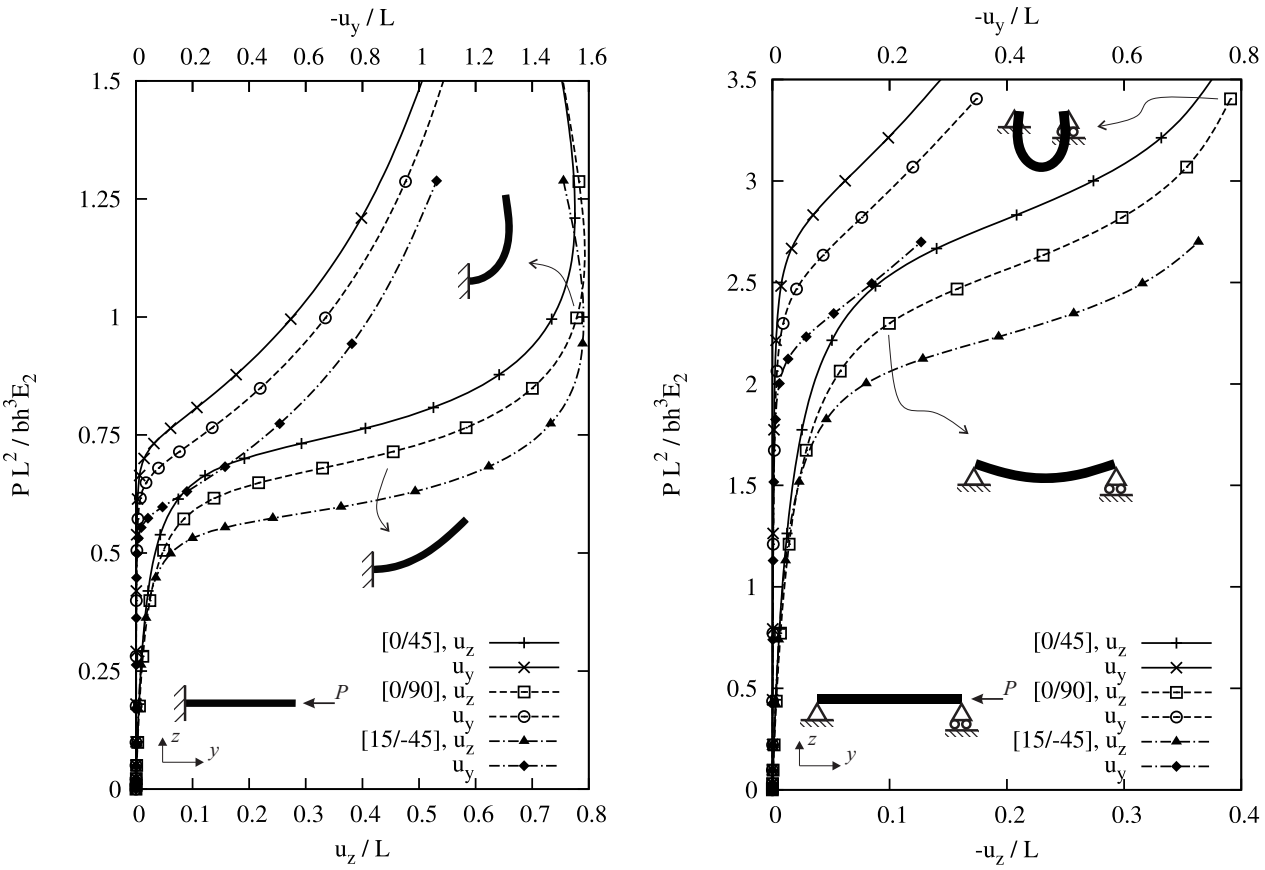

(a) Clamped-free (b) Simply-supported

Figure 9: Equilibrium curves and representative deformed states of cantilever and simply-supported two-layer asymmetric beams subjected to compression. 2L16 beam model.

L9 layer-wise kinematics provide constant and linear distributions of the shear stresses, respectively.

- The proposed beam models can provide accurate solutions with a minimum number of DOFs if compared to 3D analysis. Also, thanks to the efficiency of the proposed arc-length method, computational costs of geometrical nonlinear analysis of composite structures are extremely low.

As a second load case, the same two-layer asymmetric beam is subjected to compression loading in the analysis discussed hereinafter. Also, in order to highlight the capability of the present beam formulation to deal with arbitrary lamination angles and coupling phenomena, three different stacking sequencies are considered; namely, $[0°/90°]$, $[0°/45°]$, and $[15°/-45°]$. The equilibrium curves of the layered beams for both clamped-free and simply-supported boundary conditions are shown in Fig. 9, which provides the vertical and axial displacement components as functions of the applied compression load P according to the present 2L16 layer-wise beam model. Displacements are measured at the free end and at coordinate $x = b/3$, $z = 0$ (see Fig. 4). Some deformed states of the $[0°/90°]$ configuration are depicted in the same figure for representative purpose. In contrast, three-dimensional deformation states of the $[0°/45°]$ layered beam are shown in in Fig. 10 for different compression loadings. This figure clearly underline the possibility of this layer-wise beam formulation of facing compression/bending as well as bending/torsion couplings. Finally, for the same values of the

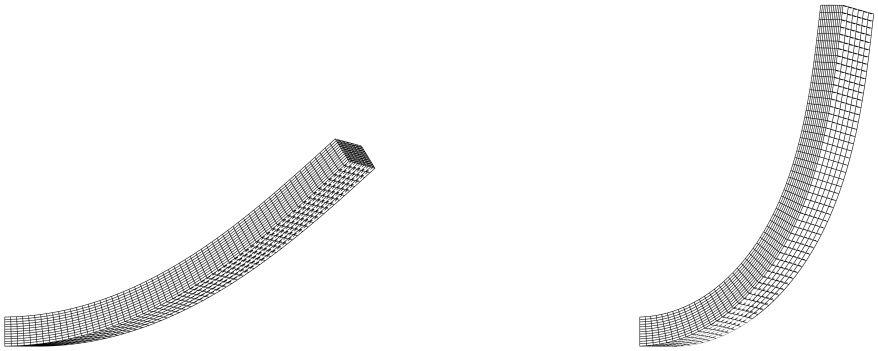

(a) $\frac{PL^2}{bh^3E_2} = 0.76,\ \frac{u_z}{L} = 0.41$ (b) $\frac{PL^2}{bh^3E_2} = 1.00,\ \frac{u_z}{L} = 0.73$

Figure 10: Three-dimensional displacement views of the cantilever $[0°/45°]$ composite beam subjected to compression. 2L16 beam model.

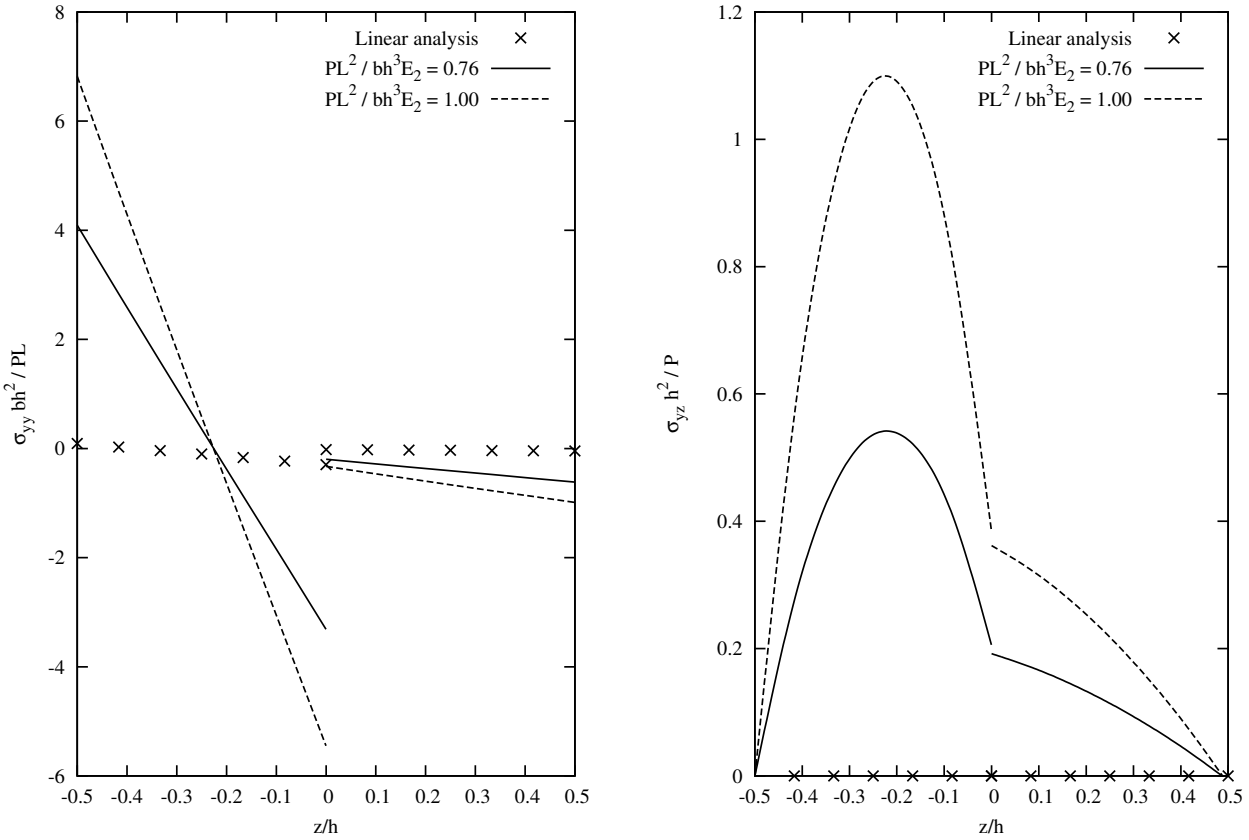

(a) σ_{yy} (b) σ_{yz}

Figure 11: Through-the-thickness distribution of axial, σ_{yy}, and transverse, σ_{yz}, stress components within linear and geometrical nonlinear ranges. $[0°/45°]$ composite beam subjected to compression and clamped-free boundary conditions. 2L16 beam model.

compression load P, through-the-thickness distributions of axial and transverse shear stresses of the [0°/45°] beam are given in Fig. 11. In this figure, geometrical nonlinear solution is compared to the linear one. The importance of taking into account nonlinear phenomena, in the case that accurate stress distribution is needed in large displacement/rotations range, is clear. Also, the layer-wise capabilities and accuracy of the present formulation are evident.

6 Conclusions

The unified formulation of geometrically nonlinear theories has been extended in this work to the analysis of laminated composite beams. By employing the Carrera Unified Formulation (CUF), the kinematics of the generic one-dimensional model has been expressed as an arbitrary expansion of the primary displacement unknowns. Subsequently, the nonlinear governing equations and the related finite element approximation have been formulated using the principle of virtual work. The complete expressions of the secant and tangent stiffness matrices of the unified beam element have been provided in terms of fundamental nuclei and in the case of laminated composite materials. Several numerical assessments have been proposed and solved by employing a Newton-Raphson linearized incremental scheme along with an arc-length constraint relationship. In detail, elastic beams with both symmetric and asymmetric stacking sequences have been considered and opportunely discussed. The results have widely demonstrated the enhanced accuracy and efficiency of the proposed method for the analysis of both post-buckling and large-deflection analyses of composite structures. Furthermore, as Lagrange expansions are employed in the domain of CUF to formulate layer-wise models, accurate stress/strain distributions can be provided with ease.

References

[1] A. Pagani and E. Carrera. Unified formulation of geometrically nonlinear refined beam theories. *Mechanics of Advanced Materials and Structures*, 2017.

[2] E. Carrera. Historical review of zig-zag theories for multilayered plates and shells. *Applied Mechanics Reviews*, 56(3):287–308, 2003.

[3] R. K. Kapania and S. Raciti. Recent advances in analysis of laminated beams and plates, Part I: Shear effects and buckling. *AIAA Journal*, 27(7):923–935, 1989.

[4] R. K. Kapania and S. Raciti. Recent advances in analysis of laminated beams and plates, Part II: Vibrations and wave propagation. *AIAA Journal*, 27(7):935–946, 1989.

[5] A. E. H. Love. *A treatise on the mathematical theory of elasticity*. Cambridge University Press, Cambridge, UK, 2013.

[6] R. Frisch-Fay. *Flexible bars*. Butterworths, Washington D.C., USA, 1962.

[7] S.P. Timoshenko and J.M. Gere. *Theory of elastic stability*. Tokyo, 1961.

[8] L. Euler. *De curvis elasticis*. Lausanne and Geneva: Bousquet, 1744.

[9] S. P. Timoshenko. On the transverse vibrations of bars of uniform cross section. *Philosophical Magazine*, 43:125–131, 1922.

[10] E. Reissner. On one-dimensional large-displacement finite-strain beam theory. *Studies in Applied Mathematics*, 52(2):87–95, 1973.

[11] E. Reissner. Some considerations on the problem of torsion and flexure of prismatical beams. *International Journal of Solids and Structures*, 15(1):41–53, 1979.

[12] E. Reissner. Further considerations on the problem of torsion and flexure of prismatical beams. *International Journal of Solids and Structures*, 19(5):385–392, 1983.

[13] R. K. Kapania and S. Raciti. Nonlinear vibrations of unsymmetrically laminated beams. *AIAA Journal*, 27(2):201–210, feb 1989.

[14] S. Agarwal, A. Chakraborty, and S. Gopalakrishnan. Large deformation analysis for anisotropic and inhomogeneous beams using exact linear static solutions. *Composite Structures*, 72(1):91–104, 2006.

[15] R. K. Gupta, J. B. Gunda, G. R. Janardhan, and G. V. Rao. Post-buckling analysis of composite beams: simple and accurate closed-form expressions. *Composite structures*, 92(8):1947–1956, 2010.

[16] D. Lanc, G. Turkalj, and I. Pesic. Global buckling analysis model for thin-walled composite laminated beam type structures. *Composite Structures*, 111:371–380, may 2014.

[17] Z.-M. Li, X.-D. Chen, and H. Wang. Exact analysis of postbuckling behavior of anisotropic composite slender beams subjected to axial compression. *Journal of Aerospace Engineering*, 27(2):318–324, mar 2014.

[18] S. Mareishi, M. Rafiee, X. Q. He, and K. M. Liew. Nonlinear free vibration, postbuckling and nonlinear static deflection of piezoelectric fiber-reinforced laminated composite beams. *Composites Part B: Engineering*, 59:123–132, mar 2014.

[19] H. Kurtaran. Geometrically nonlinear transient analysis of thick deep composite curved beams with generalized differential quadrature method. *Composite Structures*, 128:241–250, sep 2015.

[20] A. W. Obst and R. K. Kapania. Nonlinear static and transient finite element analysis of laminated beams. *Composites Engineering*, 2(5-7):375–389, 1992.

[21] G. V. Singh, G.and Rao and N. G. R. Iyengar. Nonlinear bending of thin and thick unsymmetrically laminated composite beams using refined finite element model. *Computers & structures*, 42(4):471–479, 1992.

[22] K. Chandrashekhara and K. M. Bangera. Linear and geometrically non-linear analysis of composite beams under transverse loading. *Composites science and technology*, 47(4):339–347, 1993.

[23] W. Yu, D. H. Hodges, V. V. Volovoi, and E. D. Fuchs. A generalized vlasov theory for composite beams. *Thin-Walled Structures*, 43(9):1493–1511, 2005.

[24] P. Krawczyk, F. Frey, and A. P. Zieliński. Large deflections of laminated beams with interlayer slips. *Engineering Computations*, 24(1):17–32, jan 2007.

[25] P. Krawczyk and B. Rebora. Large deflections of laminated beams with interlayer slips. *Engineering Computations*, 24(1):33–51, jan 2007.

[26] S. A. Emam. Analysis of shear-deformable composite beams in postbuckling. *Composite Structures*, 94(1):24–30, 2011.

[27] P. Vidal and O. Polit. Assessment of the refined sinus model for the non-linear analysis of composite beams. *Composite Structures*, 87:370–381, 2009.

[28] Z.-M. Li and P. Qiao. Thermal postbuckling analysis of anisotropic laminated beams with different boundary conditions resting on two-parameter elastic foundations. *European Journal of Mechanics - A/Solids*, 54:30–43, nov 2015.

[29] Z.-M. Li and P. Qiao. Buckling and postbuckling behavior of shear deformable anisotropic laminated beams with initial geometric imperfections subjected to axial compression. *Engineering Structures*, 85:277–292, feb 2015.

[30] Z.-M. Li and D.-Q. Yang. Thermal postbuckling analysis of anisotropic laminated beams with tubular cross-section based on higher-order theory. *Ocean Engineering*, 115:93–106, mar 2016.

[31] L. A. T. Mororó, A. M. C. de Melo, and E. P. Junior. Geometrically nonlinear analysis of thin-walled laminated composite beams. *Latin American Journal of Solids and Structures*, 12(11):2094–2117, nov 2015.

[32] E. Carrera, G. Giunta, and M. Petrolo. *Beam Structures: Classical and Advanced Theories*. John Wiley & Sons, 2011.

[33] E. Carrera, M. Cinefra, M. Petrolo, and E. Zappino. *Finite Element Analysis of Structures through Unified Formulation*. John Wiley & Sons, Chichester, West Sussex, UK, 2014.

[34] O. O. Ochoa and J. N. Reddy. *Finite Element Analysis of Composite Laminates*. Kluwer Academic Publishers, Dordrecht, The Netherlands, 1992.

[35] E. Carrera and M. Petrolo. Refined beam elements with only displacement variables and plate/shell capabilities. *Meccanica*, 47(3):537–556, 2012.

[36] E. Carrera and M. Petrolo. Refined one-dimensional formulations for laminated structure analysis. *AIAA Journal*, 50(1):176–189, 2012.

[37] K. J. Bathe. *Finite element procedure*. Prentice Hall, Upper Saddle River, New Jersey, USA, 1996.

[38] K. Washizu. *Variational Methods in Elasticity and Plasticity*. Pergamon, Oxford, 1968.

[39] J. N. Reddy. *An Introduction to Nonlinear Finite Element Analysis: with applications to heat transfer, fluid mechanics, and solid mechanics*. Oxford University Press, Oxford, 2014.

[40] E. Carrera. A study on arc-length-type methods and their operation failures illustrated by a simple model. *Computers & Structures*, 50(2):217–229, 1994.

[41] M. A. Crisfield. *Non-linear Finite Element Analysis of Solid and Structures*. John Wiley & Sons, Chichester, England, 1991.

[42] M. A. Crisfield. A fast incremental/iterative solution procedure that handles "snap-through". *Computers & Structures*, 13(1):55–62, 1981.

[43] M. A. Crisfield. An arc-length method including line searches and accelerations. *International journal for numerical methods in engineering*, 19(9):1269–1289, 1983.

[44] O. C. Zienkiewicz and R. L. Taylor. *The Finite Element Method for Solid and Structural Mechanics*. Butterworth-Heinemann, Washington, 6th edition, 2005.

[45] R. D. Wood and B. Schrefler. Geometrically non-linear analysis–a correlation of finite element notations. *International Journal for Numerical Methods in Engineering*, 12(4):635–642, 1978.

[46] C. Felippa and L. A. Crivelli. The core-congruential formulation of geometrically nonlinear finite elements. In P. Wriggers and W. Wagner, editors, *Non Linear Computational Mechanics. The State of the Art*. Springer, Berlin, 1991.

[47] M. Badawi and A. R. Cusens. Symmetry of the stiffness matrices for geometrically non-linear analysis. *Communications in Applied Numerical Methods*, 8(2):135–140, 1992.

[48] E. Oñate. On the derivation and possibilities of the secant stiffness matrix for non linear finite element analysis. *Computational Mechanics*, 15(6):572–593, 1995.

[49] A. Morán, E. Oñate, and J. Miquel. A general procedure for deriving symmetric expressions for the secant and tangent stiffness matrices in finite element analysis. *International Journal for Numerical Methods in Engineering*, 42(2):219–236, 1998.

[50] E. Carrera. Sull'uso dell'operatore secante in analisi non lineare di strutture multistrato con il metodo degli elementi finiti. In *XI Congresso Nazionale AIMETA, Trento*, 28 September - 2 October 1992.

[51] E. Carrera. *Comportamento Postcritico di Gusci Multistrato*. PhD thesis, Department of Aerospace Engineering, Politecnico di Torino, 1991.

Appendix A Components of the secant stiffness matrix

In this appendix, for the purpose of completeness, all the components of the secant stiffness matrix for each of the nucleus sub-matrices are given. Although the stiffness FN is given for the case of composite beam structures, it is intended that, according to Carrera *et al.*, it can be extended to the cases of plate and solid formulations with ease.

The nine components of the 3×3 fundamental nucleus of the linear stiffness matrix are provided below in the form $\mathbf{K}_0^{ij\tau s}[r,c]$, where r is the row number ($r = 1,2,3$) and c is the column number ($c = 1,2,3$).

$$
\begin{aligned}
\mathbf{K}_0^{ij\tau s}[1,1] &= < \tilde{C}_{22}\, F_{\tau,x}\, F_{s,x}\, N_i\, N_j > + < \tilde{C}_{44}\, F_{\tau,z}\, F_{s,z}\, N_i\, N_j > \\
&+ < \tilde{C}_{66}\, F_\tau\, F_s\, N_{i,y}\, N_{j,y} > + < \tilde{C}_{26}\, F_\tau\, F_{s,x}\, N_{i,y}\, N_j > \\
&+ < \tilde{C}_{26}\, F_{\tau,x}\, F_s\, N_i N_{j,y} > \\
\mathbf{K}_0^{ij\tau s}[1,2] &= < \tilde{C}_{26}\, F_{\tau,x}\, F_{s,x}\, N_i\, N_j > + < \tilde{C}_{45}\, F_{\tau,z}\, F_{s,z}\, N_i\, N_j > \\
&+ < \tilde{C}_{12}\, F_\tau\, F_{s,x}\, N_{i,y}\, N_j > + < \tilde{C}_{66}\, F_{\tau,x}\, F_s\, N_i\, N_{j,y} > \\
&+ < \tilde{C}_{16}\, F_\tau\, F_s\, N_{i,y}\, N_{j,y} > \\
\mathbf{K}_0^{ij\tau s}[1,3] &= < \tilde{C}_{44}\, F_{\tau,x}\, F_{s,z}\, N_i\, N_j > + < \tilde{C}_{23}\, F_{\tau,z}\, F_{s,x}\, N_i\, N_j > \\
&+ < \tilde{C}_{45}\, F_\tau\, F_{s,z}\, N_{i,y}\, N_j > + < \tilde{C}_{36}\, F_{\tau,z}\, F_s\, N_i\, N_{j,y} > \\
\mathbf{K}_0^{ij\tau s}[2,1] &= < \tilde{C}_{26}\, F_{\tau,x}\, F_{s,x}\, N_i\, N_j > + < \tilde{C}_{45}\, F_{\tau,z}\, F_{s,z}\, N_i\, N_j > \\
&+ < \tilde{C}_{66}\, F_\tau\, F_{s,x}\, N_{i,y}\, N_j > + < \tilde{C}_{12}\, F_{\tau,x}\, F_s\, N_i\, N_{j,y} > \\
&+ < \tilde{C}_{16}\, F_\tau\, F_s\, N_{i,y}\, N_{j,y} > \\
\mathbf{K}_0^{ij\tau s}[2,2] &= < \tilde{C}_{66}\, F_{\tau,x}\, F_{s,x}\, N_i\, N_j > + < \tilde{C}_{55}\, F_{\tau,z}\, F_{s,z}\, N_i\, N_j > \\
&+ < \tilde{C}_{11}\, F_\tau\, F_s\, N_{i,y}\, N_{j,y} > + < \tilde{C}_{16}\, F_\tau\, F_{s,x}\, N_{i,y}\, N_j > \\
&+ < \tilde{C}_{16}\, F_{\tau,x}\, F_s\, N_i\, N_{j,y} > \\
\mathbf{K}_0^{ij\tau s}[2,3] &= < \tilde{C}_{45}\, F_{\tau,x}\, F_{s,z}\, N_i\, N_j > + < \tilde{C}_{55}\, F_\tau\, F_{s,z}\, N_{i,y}\, N_j > \\
&+ < \tilde{C}_{36}\, F_{\tau,z}\, F_{s,x}\, N_i\, N_j > + < \tilde{C}_{13}\, F_{\tau,z}\, F_s\, N_i\, N_{j,y} > \\
\mathbf{K}_0^{ij\tau s}[3,1] &= < \tilde{C}_{44}\, F_{\tau,z}\, F_{s,x}\, N_i\, N_j > + < \tilde{C}_{23}\, F_{\tau,x}\, F_{s,z}\, N_i\, N_j > \\
&= < \tilde{C}_{36}\, F_\tau\, F_{s,z}\, N_{i,y}\, N_j > + < \tilde{C}_{45}\, F_{\tau,z}\, F_s\, N_i\, N_{j,y} > \\
\mathbf{K}_0^{ij\tau s}[3,2] &= < \tilde{C}_{55}\, F_{\tau,z}\, F_s\, N_i\, N_{j,y} > + < \tilde{C}_{13}\, F_\tau\, F_{s,z}\, N_{i,y}\, N_j > \\
&+ < \tilde{C}_{36}\, F_{\tau,x}\, F_{s,z}\, N_i\, N_j > + < \tilde{C}_{45}\, F_{\tau,x}\, F_{s,z}\, N_i\, N_j > \\
\mathbf{K}_0^{ij\tau s}[3,3] &= < \tilde{C}_{44}\, F_{\tau,x}\, F_{s,x}\, N_i\, N_j > + < \tilde{C}_{33}\, F_{\tau,z}\, F_{s,z}\, N_i\, N_j > \\
&+ < \tilde{C}_{55}\, F_\tau\, F_s\, N_{i,y}\, N_{j,y} > + < \tilde{C}_{45}\, F_\tau\, F_{s,x}\, N_{i,y}\, N_j > \\
&+ < \tilde{C}_{45}\, F_{\tau,x}\, F_s\, N_i\, N_{j,y} >
\end{aligned}
$$

Similarly, the components of the fundamental nucleus of the first-order nonlinear stiffness matrix $\mathbf{K}_{nll}^{ij\tau s}$ are:

For $c = 1$:

$$\begin{aligned}
\mathbf{K}_{nll}^{ij\tau s}[r,c] &= <\mathbf{u}_{,x}[r]\,\tilde{C}_{22}\,F_{\tau_{,x}}\,F_{s_{,x}}\,N_i\,N_j> + <\mathbf{u}_{,x}[r]\,\tilde{C}_{44}\,F_{\tau_{,z}}\,F_{s_{,z}}\,N_i\,N_j> \\
&+ <\mathbf{u}_{,x}[r]\,\tilde{C}_{26}\,F_{\tau_{,x}}\,F_s\,N_i\,N_{j_{,y}}> + <\mathbf{u}_{,x}[r]\,\tilde{C}_{26}\,F_\tau\,F_{s_{,x}}\,N_{i_{,y}}\,N_j> \\
&+ <\mathbf{u}_{,x}[r]\,\tilde{C}_{66}\,F_\tau\,F_s\,N_{i_{,y}}\,N_{j_{,y}}> + <\mathbf{u}_{,y}[r]\,\tilde{C}_{26}\,F_{\tau_{,x}}\,F_{s_{,x}}\,N_i\,N_j> \\
&+ <\mathbf{u}_{,y}[r]\,\tilde{C}_{45}\,F_{\tau_{,z}}\,F_{s_{,z}}\,N_i\,N_j> + <\mathbf{u}_{,y}[r]\,\tilde{C}_{66}\,F_\tau\,F_{s_{,x}}\,N_{i_{,y}}\,N_j> \\
&+ <\mathbf{u}_{,y}[r]\,\tilde{C}_{12}\,F_{\tau_{,x}}\,F_s\,N_i\,N_{j_{,y}}> + <\mathbf{u}_{,y}[r]\,\tilde{C}_{16}\,F_\tau\,F_s\,N_{i_{,y}}\,N_{j_{,y}}> \\
&+ <\mathbf{u}_{,z}[r]\,\tilde{C}_{23}\,F_{\tau_{,x}}\,F_{s_{,z}}\,N_i\,N_j> + <\mathbf{u}_{,z}[r]\,\tilde{C}_{44}\,F_{\tau_{,z}}\,F_{s_{,x}}\,N_i\,N_j> \\
&+ <\mathbf{u}_{,z}[r]\,\tilde{C}_{36}\,F_\tau\,F_{s_{,z}}\,N_{i_{,y}}\,N_j> + <\mathbf{u}_{,z}[r]\,\tilde{C}_{45}\,F_{\tau_{,z}}\,F_s\,N_i\,N_{j_{,y}}>
\end{aligned}$$

For $c = 2$:

$$\begin{aligned}
\mathbf{K}_{nll}^{ij\tau s}[r,c] &= <\mathbf{u}_{,x}[r]\,\tilde{C}_{26}\,F_{\tau_{,x}}\,F_{s_{,x}}\,N_i\,N_j> + <\mathbf{u}_{,x}[r]\,\tilde{C}_{45}\,F_{\tau_{,z}}\,F_{s_{,z}}\,N_i\,N_j> \\
&+ <\mathbf{u}_{,x}[r]\,\tilde{C}_{66}\,F_{\tau_{,x}}\,F_s\,N_i\,N_{j_{,y}}> + <\mathbf{u}_{,x}[r]\,\tilde{C}_{12}\,F_\tau\,F_{s_{,x}}\,N_{i_{,y}}\,N_j> \\
&+ <\mathbf{u}_{,x}[r]\,\tilde{C}_{16}\,F_\tau\,F_s\,N_{i_{,y}}\,N_{j_{,y}}> + <\mathbf{u}_{,y}[r]\,\tilde{C}_{66}\,F_{\tau_{,x}}\,F_{s_{,x}}\,N_i\,N_j> \\
&+ <\mathbf{u}_{,y}[r]\,\tilde{C}_{55}\,F_{\tau_{,z}}\,F_{s_{,z}}\,N_i\,N_j> + <\mathbf{u}_{,y}[r]\,\tilde{C}_{16}\,F_\tau\,F_{s_{,x}}\,N_{i_{,y}}\,N_j> \\
&+ <\mathbf{u}_{,y}[r]\,\tilde{C}_{16}\,F_{\tau_{,x}}\,F_s\,N_i\,N_{j_{,y}}> + <\mathbf{u}_{,y}[r]\,\tilde{C}_{11}\,F_\tau\,F_s\,N_{i_{,y}}\,N_{j_{,y}}> \\
&+ <\mathbf{u}_{,z}[r]\,\tilde{C}_{36}\,F_{\tau_{,x}}\,F_{s_{,z}}\,N_i\,N_j> + <\mathbf{u}_{,z}[r]\,\tilde{C}_{45}\,F_{\tau_{,z}}\,F_{s_{,x}}\,N_i\,N_j> \\
&+ <\mathbf{u}_{,z}[r]\,\tilde{C}_{13}\,F_\tau\,F_{s_{,z}}\,N_{i_{,y}}\,N_j> + <\mathbf{u}_{,z}[r]\,\tilde{C}_{55}\,F_{\tau_{,z}}\,F_s\,N_i\,N_{j_{,y}}>
\end{aligned}$$

For $c = 3$:

$$\begin{aligned}
\mathbf{K}_{nll}^{ij\tau s}[r,c] &= <\mathbf{u}_{,x}[r]\,\tilde{C}_{45}\,F_\tau\,F_{s_{,z}}\,N_{i_{,y}}\,N_j> + <\mathbf{u}_{,x}[r]\,\tilde{C}_{36}\,F_{\tau_{,z}}\,F_s\,N_i\,N_{j_{,y}}> \\
&+ <\mathbf{u}_{,x}[r]\,\tilde{C}_{44}\,F_{\tau_{,x}}\,F_{s_{,z}}\,N_i\,N_j> + <\mathbf{u}_{,x}[r]\,\tilde{C}_{23}\,F_{\tau_{,z}}\,F_{s_{,x}}\,N_i\,N_j> \\
&+ <\mathbf{u}_{,y}[r]\,\tilde{C}_{55}\,F_\tau\,F_{s_{,z}}\,N_{i_{,y}}\,N_j> + <\mathbf{u}_{,y}[r]\,\tilde{C}_{13}\,F_{\tau_{,z}}\,F_s\,N_i\,N_{j_{,y}}> \\
&+ <\mathbf{u}_{,y}[r]\,\tilde{C}_{45}\,F_{\tau_{,x}}\,F_{s_{,z}}\,N_i\,N_j> + <\mathbf{u}_{,y}[r]\,\tilde{C}_{36}\,F_{\tau_{,z}}\,F_{s_{,x}}\,N_i\,N_j> \\
&+ <\mathbf{u}_{,z}[r]\,\tilde{C}_{44}\,F_{\tau_{,x}}\,F_{s_{,x}}\,N_i\,N_j> + <\mathbf{u}_{,z}[r]\,\tilde{C}_{33}\,F_{\tau_{,z}}\,F_{s_{,z}}\,N_i\,N_j> \\
&+ <\mathbf{u}_{,z}[r]\,\tilde{C}_{45}\,F_{\tau_{,x}}\,F_s\,N_i\,N_{j_{,y}}> + <\mathbf{u}_{,z}[r]\,\tilde{C}_{45}\,F_\tau\,F_{s_{,x}}\,N_{i_{,y}}\,N_j> \\
&+ <\mathbf{u}_{,z}[r]\,\tilde{C}_{55}\,F_\tau\,F_s\,N_{i_{,y}}\,N_{j_{,y}}>
\end{aligned}$$

The components of $\mathbf{K}_{lnl}^{ij\tau s}$ are not given here, but they can be easily obtained from $\mathbf{K}_{nll}^{ij\tau s}$. In fact, it is clear from Eq. (24) that $\left(\mathbf{K}_{lnl}^{ij\tau s}\right)^T = \frac{1}{2}\mathbf{K}_{nll}^{ij\tau s}$.

Finally, the generic component $[r, c]$ of the matrix $\mathbf{K}^{ij\tau s}_{nlnl}$ is summarized in the following:

$$
\begin{aligned}
2 \times \mathbf{K}^{ij\tau s}_{nlnl}[r,c] \;=\; & < \mathbf{u}_{,x}[r]\, \mathbf{u}_{,x}[c]\; \tilde{C}_{22}\, F_{\tau,_x}\, F_{s,_x}\, N_i\, N_j > + < \mathbf{u}_{,x}[r]\, \mathbf{u}_{,x}[c]\, \tilde{C}_{44}\, F_{\tau,_z}\, F_{s,_z}\, N_i\, N_j > \\
+ \; & < \mathbf{u}_{,x}[r]\, \mathbf{u}_{,x}[c]\, \tilde{C}_{66}\, F_\tau\, F_s\, N_{i,_y}\, N_{j,_y} > + < \mathbf{u}_{,x}[r]\, \mathbf{u}_{,x}[c]\, \tilde{C}_{26}\, F_\tau\, F_{s,_x}\, N_{i,_y}\, N_j > \\
+ \; & < \mathbf{u}_{,x}[r]\, \mathbf{u}_{,x}[c]\, \tilde{C}_{26,_x}\, F_\tau\, F_s\, N_i\, N_{j,_y} > + < \mathbf{u}_{,y}[r]\, \mathbf{u}_{,y}[c]\; \tilde{C}_{66}\, F_{\tau,_x}\, F_{s,_x}\, N_i\, N_j > \\
+ \; & < \mathbf{u}_{,y}[r]\, \mathbf{u}_{,y}[c]\, \tilde{C}_{55}\, F_{\tau,_z}\, F_{s,_z}\, N_i\, N_j > + < \mathbf{u}_{,y}[r]\, \mathbf{u}_{,y}[c]\, \tilde{C}_{11}\, F_\tau\, F_s\, N_{i,_y}\, N_{j,_y} > \\
+ \; & < \mathbf{u}_{,y}[r]\, \mathbf{u}_{,y}[c]\, \tilde{C}_{16}\, F_\tau\, F_{s,_x}\, N_{i,_y}\, N_j > + < \mathbf{u}_{,y}[r]\, \mathbf{u}_{,y}[c]\, \tilde{C}_{16}\, F_{\tau,_x}\, F_s\, N_i\, N_{j,_y} > \\
+ \; & < \mathbf{u}_{,z}[r]\, \mathbf{u}_{,z}[c]\; \tilde{C}_{44}\, F_{\tau,_x}\, F_{s,_x}\, N_i\, N_j > + < \mathbf{u}_{,z}[r]\, \mathbf{u}_{,z}[c]\, \tilde{C}_{33}\, F_{\tau,_z}\, F_{s,_z}\, N_i\, N_j > \\
+ \; & < \mathbf{u}_{,z}[r]\, \mathbf{u}_{,z}[c]\, \tilde{C}_{55}\, F_\tau\, F_s\, N_{i,_y}\, N_{j,_y} > + < \mathbf{u}_{,z}[r]\, \mathbf{u}_{,z}[c]\, \tilde{C}_{45}\, F_\tau\, F_{s,_x}\, N_{i,_y}\, N_j > \\
+ \; & < \mathbf{u}_{,z}[r]\, \mathbf{u}_{,z}[c]\, \tilde{C}_{45}\, F_{\tau,_x}\, F_s\, N_i\, N_{j,_y} > + < \mathbf{u}_{,x}[r]\, \mathbf{u}_{,y}[c]\, \tilde{C}_{12}\, F_\tau\, F_{s,_x}\, N_{i,_y}\, N_j > \\
+ \; & < \mathbf{u}_{,x}[r]\, \mathbf{u}_{,y}[c]\, \tilde{C}_{66}\, F_{\tau,_x}\, F_s\, N_i\, N_{j,_y} > + < \mathbf{u}_{,x}[r]\, \mathbf{u}_{,y}[c]\, \tilde{C}_{26}\, F_{\tau,_x}\, F_{s,_x}\, N_i\, N_j > \\
+ \; & < \mathbf{u}_{,x}[r]\, \mathbf{u}_{,y}[c]\, \tilde{C}_{45}\, F_{\tau,_z}\, F_{s,_z}\, N_i\, N_j > + < \mathbf{u}_{,x}[r]\, \mathbf{u}_{,y}[c]\, \tilde{C}_{16}\, F_\tau\, F_s\, N_{i,_y}\, N_{j,_y} > \\
+ \; & < \mathbf{u}_{,y}[r]\, \mathbf{u}_{,x}[c]\, \tilde{C}_{26}\, F_{\tau,_x}\, F_{s,_x}\, N_i\, N_j > + < \mathbf{u}_{,y}[r]\, \mathbf{u}_{,x}[c]\, \tilde{C}_{45}\, F_{\tau,_z}\, F_{s,_z}\, N_i\, N_j > \\
+ \; & < \mathbf{u}_{,y}[r]\, \mathbf{u}_{,x}[c]\, \tilde{C}_{16}\, F_\tau\, F_s\, N_{i,_y}\, N_{j,_y} > + < \mathbf{u}_{,y}[r]\, \mathbf{u}_{,x}[c]\, \tilde{C}_{12}\, F_{\tau,_x}\, F_s\, N_i\, N_{j,_y} > \\
+ \; & < \mathbf{u}_{,y}[r]\, \mathbf{u}_{,x}[c]\, \tilde{C}_{66}\, F_\tau\, F_{s,_x}\, N_{i,_y}\, N_j > + < \mathbf{u}_{,x}[r]\, \mathbf{u}_{,z}[c]\, \tilde{C}_{23}\, F_{\tau,_z}\, F_{s,_x}\, N_i\, N_j > \\
+ \; & < \mathbf{u}_{,x}[r]\, \mathbf{u}_{,z}[c]\, \tilde{C}_{44}\, F_{\tau,_x}\, F_{s,_z}\, N_i\, N_j > + < \mathbf{u}_{,x}[r]\, \mathbf{u}_{,z}[c]\, \tilde{C}_{45}\, F_\tau\, F_{s,_z}\, N_{i,_y}\, N_j > \\
+ \; & < \mathbf{u}_{,x}[r]\, \mathbf{u}_{,z}[c]\, \tilde{C}_{36}\, F_{\tau,_z}\, F_s\, N_i\, N_{j,_y} > + < \mathbf{u}_{,z}[r]\, \mathbf{u}_{,x}[c]\, \tilde{C}_{23}\, F_{\tau,_x}\, F_{s,_z}\, N_i\, N_j > \\
+ \; & < \mathbf{u}_{,z}[r]\, \mathbf{u}_{,x}[c]\, \tilde{C}_{44}\, F_{\tau,_z}\, F_{s,_x}\, N_i\, N_j > + < \mathbf{u}_{,z}[r]\, \mathbf{u}_{,x}[c]\, \tilde{C}_{36}\, F_\tau\, F_{s,_z}\, N_{i,_y}\, N_j > \\
+ \; & < \mathbf{u}_{,z}[r]\, \mathbf{u}_{,x}[c]\, \tilde{C}_{45}\, F_{\tau,_z}\, F_s\, N_i\, N_{j,_y} > + < \mathbf{u}_{,y}[r]\, \mathbf{u}_{,z}[c]\, \tilde{C}_{13}\, F_{\tau,_z}\, F_s\, N_i\, N_{j,_y} > \\
+ \; & < \mathbf{u}_{,y}[r]\, \mathbf{u}_{,z}[c]\, \tilde{C}_{55}\, F_\tau\, F_{s,_z}\, N_{i,_y}\, N_j > + < \mathbf{u}_{,y}[r]\, \mathbf{u}_{,z}[c]\, \tilde{C}_{45}\, F_{\tau,_x}\, F_{s,_z}\, N_i\, N_j > \\
+ \; & < \mathbf{u}_{,y}[r]\, \mathbf{u}_{,z}[c]\, \tilde{C}_{36}\, F_{\tau,_z}\, F_{s,_x}\, N_i\, N_j > + < \mathbf{u}_{,z}[r]\, \mathbf{u}_{,y}[c]\, \tilde{C}_{55}\, F_{\tau,_z}\, F_s\, N_i\, N_{j,_y} > \\
+ \; & < \mathbf{u}_{,z}[r]\, \mathbf{u}_{,y}[c]\, \tilde{C}_{13}\, F_\tau\, F_{s,_z}\, N_{i,_y}\, N_j > + < \mathbf{u}_{,z}[r]\, \mathbf{u}_{,y}[c]\, \tilde{C}_{36}\, F_{\tau,_x}\, F_{s,_z}\, N_i\, N_j > \\
+ \; & < \mathbf{u}_{,z}[r]\, \mathbf{u}_{,y}[c]\, \tilde{C}_{45}\, F_{\tau,_z}\, F_{s,_x}\, N_i\, N_j >
\end{aligned}
$$

In the expressions above, $\mathbf{u}_{,x}[r]$ represents the r-th component of the vector $\dfrac{\partial \mathbf{u}}{\partial x}$; e.g. $\mathbf{u}_{,x}[2] = u_{y,_x}$. Analogously, $\mathbf{u}_{,y}[c]$ is the c-th component of the vector $\dfrac{\partial \mathbf{u}}{\partial y}$, etc.